Supplementary Material for 'Inertio-elastic instability of a vortex column'

1. Elastic Rayleigh Equation: the continuous spectra

The elastic Rayleigh equation as derived in the main text is given by,

$$D\left[r^3 P D\xi\right] = r(m^2-1)P\xi, \tag{1.1}$$

where $P = \Sigma^2 - 2m^2\mathrm{E}\Omega'^2$. In contrast to the inviscid Rayleigh operator which supports a single continuous spectrum ranging over the base-state interval of angular velocities (Case (1960);Roy & Subramanian (2014*a*);Roy & Subramanian (2014*b*)), the elastic Rayleigh operator supports three distinct continuous spectra. The first of these is the original inviscid continuous spectrum modified by elasticity. There exist in addition a pair of continuous spectra associated with fore- and aft-travelling elastic shear waves in the azimuthal direction. On writing $\Sigma^2 - 2m^2\mathrm{E}\Omega'^2$ in (1.1) as $(\Sigma + m\Omega'\sqrt{2\mathrm{E}})(\Sigma - m\Omega'\sqrt{2\mathrm{E}})$, it is seen that these shear waves propagate at angular frequencies of $\pm(m\Omega')\sqrt{2\mathrm{E}}$ relative to the base-state angular frequency, $m\Omega(r)$, at r. Unlike the finite-De continuous spectra discussed in section 2 of the main text, these elastic-Rayleigh travelling-wave spectra arise due to a balance of the inertial and elastic terms, and must therefore disappear for any finite De. Thus, in the presence of any amount of relaxation, the original travelling-wave CS-modes are no longer true eigenfunctions, and must instead be expressible in terms of a superposition of finite De discrete modes. Aside from the obvious reduction in the order of the equation, this again highlights the singular relation between the spectrum of the elastic Rayleigh equation discussed below and the finite De spectrum, spectrum associated with the viscoelastic Orr-Sommerfeld equation.

The elastic Rayleigh equation for arbitrary E belongs to the confluent Heun class with a pair of regular singular points at the travelling wave locations given by $\Sigma \pm m\Omega'\sqrt{2\mathrm{E}} = 0$, and an irregular one at infinity (Slavyanov & Lay (2000)). The associated insolubility implies that we only analyze the continuous spectra for small but finite E. The inertial terms become arbitrarily small sufficiently close to the critical radius, defined by $\Sigma(r_c) = 0$, and for any E however small, the effects of elasticity become comparable to those of inertia in a boundary layer around r_c. Thus, the elastic continuous spectra are analyzed below via a matched asymptotic expansions approach which involves matching the leading-order inviscid solutions, in regions away from r_c, to those in an $O(\mathrm{E}^{\frac{1}{2}})$ interior elastic boundary layer around the critical radius. The analysis of the continuous spectrum lends additional insight into the structure of the unstable (discrete) mode described in detail in the next section. The discrete mode mirrors the structure of the elastic CS-modes in the limit of a vanishingly small growth rate.

To begin with, we summarize briefly the inviscid 2D CS-spectrum of the Rankine vortex for $\mathrm{E} = 0$ as found by Roy & Subramanian (2014), and referred to as the Λ_1-family therein. In light of the scalings used in section 2 of the main text, the non-dimensional angular velocity profile for the Rankine vortex is given by $\Omega(r) = \mathcal{H}(1-r) + \frac{1}{r^2}\mathcal{H}(r-1)$,

$\mathcal{H}(z)$ being the Heaviside function. For an azimuthal wavenumber m, the 2D CS-modes span the angular frequency range $(0, m\Omega_0)$, and have a twin-vortex-sheet structure. The vortex sheets are cylindrical, being threaded by axial lines, with one sheet located at the edge of the core and the other at the critical radius in the irrotational exterior. A given CS-mode rotates with the base-angular velocity corresponding to the critical radius. Therefore, the radial velocity and axial vorticity eigenfunctions are of the form $[u_r(r;r_c), w_z(r;r_c)] = [\hat{u}_r(r;r_c); \hat{w}_z(r;r_c)]e^{\mathrm{i}(m\theta-\omega t)}$ with $\omega = \Omega(r_c)$, $r_c = (m/\omega)^{\frac{1}{2}}$, and

$$\hat{u}_r(r;r_c) = dr^{m-1} \qquad r < 1, \tag{1.2}$$

$$= c_1 r^{m-1} + c_2 \frac{1}{r^{m+1}} \qquad 1 < r < r_c, \tag{1.3}$$

$$= \frac{1}{r_c}\frac{1}{r^{m+1}} \qquad r > r_c, \tag{1.4}$$

$$\hat{w}_z(r;r_c) = \big[\frac{2\mathrm{i}d}{(\omega - m)}\,\delta(r-1) - A(r_c)\delta(r-r_c)\big], \tag{1.5}$$

where

$$d = \frac{1}{r_c} + \frac{\mathrm{i}A(r_c)}{2}\left[r_c^{m+1} - \frac{1}{r_c^{m-1}}\right], \tag{1.6}$$

$$c_1 = -\frac{\mathrm{i}A(r_c)}{2}\frac{1}{r_c^{m-1}}, \tag{1.7}$$

$$c_2 = \frac{1}{r_c} + \frac{\mathrm{i}A(r_c)}{2} r_c^{m+1}, \tag{1.8}$$

$$A(r_c) = \frac{(2\mathrm{i}/r_c)[(m-1)-\omega]}{(1/r_c^{m-1}) + [(m-1)-\omega]r_c^{m+1}}. \tag{1.9}$$

The radial velocity eigenfunction itself is continuous at $r = r_c$, but the discontinuities in slope at both $r = 1$ and $r = r_c$ correspond to delta-function (vortex-sheet) contributions in the perturbation axial vorticity field. The first delta function is an artifact of the kink in the base-state (Rankine) profile, and it is the amplitude of the second vortex sheet, $A(r_c)$, that is of interest and that characterizes the 2D CS-spectrum. Note that $A(r_c)$, and therefore c_1, equals zero when $\omega = (m-1)$, which corresponds to the regular Kelvin mode with a critical radius given by $r_{ck} = (\frac{m}{m-1})^{\frac{1}{2}}$; the radial velocity in the exterior now monotonically decays as $1/r^{(m+1)}$. There is a direct analogy between the 2D CS-spectra of plane Couette flow as found by Case (1960) and that of the Rankine vortex summarized above. In both cases, the vorticity eigenfunctions are vortex-sheets convected with the base-state flow - a single plane vortex sheet for Couette flow and a pair of cylindrical sheets for the Rankine vortex. The crucial difference is the additional presence of the Kelvin mode above in the latter case. While the inviscid spectrum for plane Couette flow (and other non-inflectional profiles) is purely continuous with the amplitude of the vortex-sheet remaining non-zero over the entire range of wave speeds, there exists a unique angular frequency, the Kelvin mode for a given m, for which the vortex-sheet amplitude is zero for the case of the Rankine vortex.

For a Rankine vortex, the Kelvin mode, together with the 2D CS-modes, provide a complete basis for an arbitrary axial vorticity field in two dimensions (Roy & Subramanian 2014*b*). For almost any initial axial vorticity field, the linearized temporal evolution (of the kinetic energy or other integral measures), for a Rankine vortex, is characterized by a long-time algebraic decay characteristic of the inviscid continuous spectrum; the

exception is an initial condition localized at the critical radius which excites the Kelvin mode. In contrast, the absence of a regular discrete mode for non-compact Rankine-like profiles, (the analog of the inviscid regular Kelvin mode is now a vorticity eigenfunction with a Cauchy-principal-value singularity at the critical radius) implies that the temporal evolution, for initial conditions localized at the critical radius, involves an intermediate asymptotic regime characterized by an exponential decaying quasi-mode, the decay rate being proportional to the (small) vorticity gradient at the critical radius. In the linearized approximation, this exponential decay is followed by an algebraic decay, as for a Rankine vortex; nonlinear effects, however, lead to a finite-amplitude tripolar structure (Balmforth *et al.* 2013; Schecter *et al.* 2000; Balmforth *et al.* 2001; Pradeep & Hussain 2006).

Returning to the Rankine vortex for small but finite E, we examine the solutions of (1.1) separately in the outer region where $r - r_c \sim O(1)$, and in the inner region (the elastic boundary layer) where $r - r_c \sim O(\mathrm{E}^{\frac{1}{2}})$, before matching them to determine the unknown coefficients in the respective domains. We assume the critical radius, r_c, to be such that the elastic boundary layer lies an $O(1)$ distance away from the edge of the core ($r = 1$). The solutions in the outer regions, at leading order, are thus identical to those given in (1.2)-(1.4) except that (1.3) and (1.4) are not valid right until r_c. Likewise, apart from the core contribution (the term proportional to $\delta(r-1)$ in (1.5)), the vorticity field is localized in the elastic boundary layer around r_c, although no longer a delta function at this location. Thus, (1.3) is now valid in the range $r > 1, (r_c - r) \gg O(\mathrm{E}^{\frac{1}{2}})$ while (1.4) is now valid in the range $(r - r_c) \gg O(\mathrm{E}^{\frac{1}{2}})$. Note that since $P = \Sigma^2 - 2m^2\mathrm{E}\Omega'^2$ in (1.1), the direct effect of elasticity enters the outer regions only at $O(\mathrm{E})$. At $O(\mathrm{E}^{\frac{1}{2}})$, the outer solutions still satisfy the inviscid Rayleigh equation, and the effects of elasticity only enter via matching to the far-field forms of the elastic boundary layer solution. For purposes of matching below, it is convenient to normalize the perturbation in the core region, so that $\hat{u}_r(r; r_c) = r^{m-1}$ for $r < 1$ instead of (1.2) (this being valid to all orders in E). As a result, instead of (1.3) and (1.4), we have:

$$\hat{u}_{r1}(r; r_c) = c_1^{(0)} r^{m-1} + \frac{(1-c_1^{(0)})}{r^{m+1}} + \mathrm{E}^{\frac{1}{2}} c_1^{(1)} (r^{m-1} - \frac{1}{r^{m+1}}) + O(\mathrm{E}) \quad r > 1, r_c - r \gg O(\mathrm{E}^{\frac{1}{2}}), \tag{1.10}$$

$$\hat{u}_{r2}(r; r_c) = \frac{c_2^{(0)} + \mathrm{E}^{\frac{1}{2}} c_2^{(1)}}{r^{m+1}} + O(\mathrm{E}) \qquad r - r_c \gg O(\mathrm{E}^{\frac{1}{2}}), \tag{1.11}$$

for the irrotational radial velocity perturbation outside the core and outside the elastic boundary layer. The choice of constant in (1.10) reflects consistency with the normalized core perturbation at $r = 1$. Since one is looking for elastic generalizations of the Λ_1 CS-modes, we also impose continuity of the radial velocity for $r \to r_c$, as seen from the outer region. This implies $c_1^{(0)} r_c^{m-1} + \frac{(1-c_1^{(0)})}{r_c^{m+1}} = \frac{c_2^{(0)}}{r_c^{m+1}} = \hat{u}_r(r_c; r_c)$, which also leads to the relation between the two constants involved: $c_2^{(0)} = c_1^{(0)}(r_c^{2m} - 1) + 1$.

It may be shown that a balance between the inertial and elastic terms occurs at leading order when $r - r_c \sim O(\mathrm{E}^{\frac{1}{2}})$, and one therefore defines the boundary layer variable $\eta = \frac{r - r_c}{(2\mathrm{E})^{\frac{1}{2}}}$. On using the expansion $\Sigma(r) \approx -m\Omega_c'(r - r_c) - m\Omega_c'' \frac{(r-r_c)^2}{2} \approx -m\Omega_c'(2\mathrm{E})^{\frac{1}{2}}\eta[1 + \frac{\Omega_c''}{\Omega_c'}(\frac{\mathrm{E}}{2})^{\frac{1}{2}}\eta]$, the original relationship between the radial velocity and displacement, $\xi(r) = (\mathrm{i}\hat{u}_r)/\Sigma(r)$, takes the form $\tilde{u}_r(\eta) = -\mathrm{i}m\Omega_c'\eta[1 + \frac{\Omega_c''}{\Omega_c'}(\frac{\mathrm{E}}{2})^{\frac{1}{2}}\eta]\tilde{\xi}(\eta)$ in the boundary layer, to

$O(\mathrm{E})$, with $\xi(r) = (2\mathrm{E})^{\frac{1}{2}}\tilde{\xi}(\eta)$. Further, $P = (\omega - m\Omega(r))^2 - 2m^2\mathrm{E}[\Omega'(r)]^2 \approx 2m^2\mathrm{E}{\Omega'_c}^2[\eta^2 - 1 + \frac{\Omega''_c}{\Omega'_c}(2\mathrm{E})^{\frac{1}{2}}\eta^3]$. To $O(\mathrm{E}^{\frac{1}{2}})$, the governing equation, (1.1), then takes the form:

$$\frac{d}{d\eta}\left[\{r_c + (2\mathrm{E})^{\frac{1}{2}}\eta\}^3\left[(\eta^2-1) - \frac{3\sqrt{2}}{r_c}\mathrm{E}^{\frac{1}{2}}\right]\frac{d\tilde{\xi}}{d\eta}\right] = O(\mathrm{E}), \tag{1.12}$$

in terms of the re-scaled radial displacement, $\tilde{\xi}(\eta)$, in the boundary layer. Here, we have used that $\Omega'_c = -\frac{2}{r_c^3}, \Omega''_c = \frac{6}{r_c^4}$ for a Rankine vortex. The form of (1.12) evidently suggests a series expansion of the form $\tilde{\xi}(\eta) = \tilde{\xi}^{(0)}(\eta) + \mathrm{E}^{\frac{1}{2}}\tilde{\xi}^{(1)}(\eta) + O(\mathrm{E})$, and one obtains the following governing equations at $O(1)$ and $O(\mathrm{E}^{\frac{1}{2}})$, respectively:

$$\frac{d}{d\eta}\left[(\eta^2-1)\frac{d\tilde{\xi}^{(0)}}{d\eta}\right] = 0, \tag{1.13}$$

$$\frac{d}{d\eta}\left[(\eta^2-1)\frac{d\tilde{\xi}^{(1)}}{d\eta}\right] = \frac{3\sqrt{2}}{r_c}\frac{d}{d\eta}\left[\eta\frac{d\tilde{\xi}^{(0)}}{d\eta}\right]. \tag{1.14}$$

The solution of (1.13) is given by:

$$\tilde{\xi}^{(0)}(\eta) = A_1^{(0)} + A_2^{(0)}\ln|\frac{\eta-1}{\eta+1}|, \tag{1.15}$$

implying a radial velocity in the boundary layer of the form:

$$\tilde{u}_r^{(0)}(\eta) = -\mathrm{i}m\Omega'_c\eta\left[A_1^{(0)} + A_2^{(0)}\ln|\frac{\eta-1}{\eta+1}|\right], \tag{1.16}$$

at leading order. The values $\eta = \pm 1$ denote the locations of the travelling wave singularities where the radial velocity is logarithmically divergent. This divergence is expected since the Frobenius exponents associated with each of the regular singularities are both 0. The singularities divide the boundary layer into three regions, with the solution forms in the individual regions may be written explicitly as:

$$\tilde{u}_{r-}^{(0)}(\eta) = \eta\left[\hat{A}_{1-}^{(0)} + \hat{A}_2^{(0)}\ln\frac{\eta-1}{\eta+1}\right] \qquad \eta < -1, \tag{1.17}$$

$$\tilde{u}_r^{(0)}(\eta) = \eta\left[\hat{A}_1^{(0)} + \hat{A}_2^{(0)}\ln\frac{1-\eta}{1+\eta}\right] \qquad -1 < \eta < 1, \tag{1.18}$$

$$\tilde{u}_{r+}^{(0)}(\eta) = \eta\left[\hat{A}_{1+}^{(0)} + \hat{A}_2^{(0)}\ln\frac{\eta-1}{\eta+1}\right] \qquad \eta > 1, \tag{1.19}$$

where $\hat{A}_i^{(0)} = -\mathrm{i}m\Omega'_cA_i^{(0)}$. Note that we have chosen the same constant for the singular logarithmic solution in all three parts of the boundary layer with the logarithm being real valued in each region (this being possible by suitable choice of the regular constants). Such a choice is consistent with the purely inviscid case ($\mathrm{E} = 0$) where, for a general non-linear shear flow, the constant multiplying the logarithmically singular Tollmein solution is the same across the critical level, and it is the jump in the constant multiplying the regular solution that generates the inviscid CS-spectrum of the Rayleigh equation (Balmforth & Morrison (1995a)). It will be seen below that the constants in the two peripheral regions ($\hat{A}_{1\pm}^{(0)}$,$\hat{A}_2^{(0)}$) are constrained by matching, and an appropriate choice can accommodate the differing slopes of the outer solutions on either side. The regular constant in the central part of the boundary layer, at leading ($\hat{A}_1^{(0)}$) and higher orders, can be chosen independently, however, and this additional degree of freedom is

crucial to the existence of additional continuous spectra for any finite E.

Using (1.15) in (1.14), and solving, gives:

$$\tilde{\xi}^{(1)}(\eta) = A_1^{(1)} + \left[A_2^{(1)} + \frac{3A_2^{(0)}}{\sqrt{2}r_c}\eta\right]\ln|\frac{\eta-1}{\eta+1}| - \frac{3\sqrt{2}A_2^{(0)}}{r_c}\frac{1}{\eta^2-1}, \tag{1.20}$$

where the terms proportional to $A_1^{(1)}$ and $A_2^{(1)}$ denote the homogeneous solution. Although not made explicit in (1.20), a distinction will again being made between solution forms in the the three parts of the elastic boundary layer similar to that done at leading order. The radial velocity in the elastic boundary layer, at $O(\mathrm{E}^{\frac{1}{2}})$, is given by:

$$\tilde{u}_r^{(1)}(\eta) = \eta\left[\hat{A}_1^{(1)} + \left(\hat{A}_2^{(1)} + \frac{3\hat{A}_2^{(0)}}{\sqrt{2}r_c}\eta\right)\ln|\frac{\eta-1}{\eta+1}| - \frac{3\sqrt{2}\hat{A}_2^{(0)}}{r_c}\frac{1}{\eta^2-1}\right], \tag{1.21}$$

where $\hat{A}_i^{(1)} = -\mathrm{i}m\Omega_c' A_i^{(1)}$.

The matching requirement between the outer regions and the elastic boundary layer may be stated as: $\lim_{r\to r_c}\hat{u}_{r1}(r;r_c) = \lim_{\eta\to-\infty}\tilde{u}_{r-}(\eta)$ and $\lim_{r\to r_c}\hat{u}_{r2}(r;r_c) = \lim_{\eta\to\infty}\tilde{u}_{r+}(\eta)$ to $O(\mathrm{E}^{\frac{1}{2}})$. As pointed out earlier, the only difference between the 2D inviscid spectra of plane Couette flow and the Rankine vortex is the existence of a lone discrete mode - the Kelvin mode - in the latter case. In order to discriminate between the generalizations of the inviscid CS-modes and the Kelvin mode for non-zero E, one needs to carry out the matching to $O(\mathrm{E}^{\frac{1}{2}})$. At $O(1)$, the matching process ensures the continuity of the radial velocity across the elastic boundary layer, and it is only at $O(\mathrm{E}^{\frac{1}{2}})$ that the two ends of the elastic boundary layer ($\eta\to\pm\infty$) sense the difference in the slopes of the outer eigenfunctions, $\hat{u}_{r1}(r;r_c)$ and $\hat{u}_{r2}(r;r_c)$, for r approaching r_c. It is precisely this jump in slope that differentiates the CS-modes from the Kelvin mode.

The far-field forms of the solutions in the peripheral regions of the elastic boundary layer are given by:

$$\lim_{\eta\to\pm\infty}\tilde{u}_{r-}(\eta) = \hat{A}_{1\pm}^{(0)}\eta - 2\hat{A}_2^{(0)} + \mathrm{E}^{\frac{1}{2}}\left[-2\hat{A}_2^{(1)} + \left(\hat{A}_{1\pm}^{(1)} - \frac{3\sqrt{2}}{r_c}\hat{A}_2^{(0)}\right)\eta\right], \tag{1.22}$$

where the neglected terms only affect the matching at $o(\mathrm{E}^{\frac{1}{2}})$. The above expressions are to be matched to the limiting forms of the outer solutions obtained from (1.10) and (1.11) in the limit $r\to r_c + (2\mathrm{E})^{\frac{1}{2}}\eta$, which are given by:

$$\hat{u}_{r1}(r;r_c) = \hat{u}_r(r_c;r_c) + \mathrm{E}^{\frac{1}{2}}\left[\left(c_1^{(0)}(m-1)r_c^{m-2} - \frac{(m+1)(1-c_1^{(0)})}{r_c^{m+2}}\right)\sqrt{2}\eta + c_1^{(1)}(r_c^{m-1} - \frac{1}{r_c^{m+1}})\right] + O(\mathrm{E}), \tag{1.23}$$

$$\hat{u}_{r2}(r;r_c) = \hat{u}_r(r_c;r_c) + \mathrm{E}^{\frac{1}{2}}\left[-\frac{\sqrt{2}(m+1)c_2^{(0)}}{r_c^{m+2}}\eta + \frac{c_2^{(1)}}{r_c^{m+1}}\right] + O(\mathrm{E}). \tag{1.24}$$

Matching (1.22) and (1.23)-(1.24), at leading order, gives $\hat{A}_{1\pm}^{(0)} = 0$ and $\hat{A}_2^{(0)} = -\frac{\hat{u}_r(r_c;r_c)}{2}$. A consistent match of the constant term at $O(\mathrm{E}^{\frac{1}{2}})$ gives $\hat{A}_2^{(1)} = c_1^{(1)} = c_2^{(1)} = 0$. Matching

the term proportional to η at $O(\mathrm{E}^{\frac{1}{2}})$ gives:

$$\hat{A}_{1-}^{(1)} = \frac{3\sqrt{2}}{r_c}\hat{A}_2^{(0)} + \sqrt{2}\left(c_1^{(0)}(m-1)r_c^{m-2} - \frac{(m+1)(1-c_1^{(0)})}{r_c^{m+2}}\right), \tag{1.25}$$

$$= -\frac{3}{\sqrt{2}r_c}\hat{u}_r(r_c;r_c) + \sqrt{2}\left[\frac{(m-1)r_c^{2m} + (m+1)}{r_c^{m+2}}\frac{r_c^{m+1}\hat{u}_r(r_c;r_c) - 1}{r_c^{2m} - 1} - \frac{m+1}{r_c^{m+2}}\right], \tag{1.26}$$

$$\hat{A}_{1+}^{(1)} = \frac{3\sqrt{2}}{r_c}\hat{A}_2^{(0)} - \frac{(m+1)\sqrt{2}}{r_c^{m+2}}\,c_2^{(0)}, \tag{1.27}$$

$$= -\frac{(2m+5)}{\sqrt{2}r_c}\hat{u}_r(r_c;r_c), \tag{1.28}$$

where the two boundary-layer constants are rewritten in terms of $\hat{u}_r(r_c;r_c)$, the amplitude of the radial velocity eigenfunction at the critical radius.

Having determined the constants above, the forms of the eigenfunction in the outer regions, to $O(\mathrm{E}^{\frac{1}{2}})$, are given by:

$$\hat{u}_{r1}(r;r_c) = c_1^{(0)}r^{m-1} + \frac{(1-c_1^{(0)})}{r^{m+1}}; \qquad \hat{u}_{r2}(r;r_c) = \frac{c_2^{(0)}}{r^{m+1}}, \tag{1.29}$$

where $c_1^{(0)}$ and $c_2^{(0)}$ have been defined in terms $\hat{u}_r(r_c;r_c)$ above. The form of the eigenfunction within the elastic boundary layer may be written down in the following piecewise form:

$$\tilde{u}_{r-}(\eta) = \hat{A}_2^{(0)}\mathrm{Pf.}\eta\ln\frac{\eta-1}{\eta+1} + \mathrm{E}^{\frac{1}{2}}\eta\left[\hat{A}_{1-}^{(1)} + \frac{3}{\sqrt{2}r_c}\hat{A}_2^{(0)}\mathrm{Pf.}\left(\eta\ln\frac{\eta-1}{\eta+1} - \frac{2}{\eta^2-1}\right)\right] \qquad \eta < -1, \tag{1.30}$$

$$\tilde{u}_r(\eta) = \eta\left[\hat{A}_1 + \hat{A}_2^{(0)}\mathrm{Pf.}\ln\frac{1-\eta}{1+\eta}\right] + \mathrm{E}^{\frac{1}{2}}\eta\left[\frac{3}{\sqrt{2}r_c}\hat{A}_2^{(0)}\mathrm{Pf.}\left(\eta\ln\frac{1-\eta}{1+\eta} - \frac{2}{\eta^2-1}\right)\right] \qquad -1 < \eta < -1, \tag{1.31}$$

$$\tilde{u}_{r+}(\eta) = \hat{A}_2^{(0)}\mathrm{Pf.}\eta\ln\frac{\eta-1}{\eta+1} + \mathrm{E}^{\frac{1}{2}}\eta\left[\hat{A}_{1+}^{(1)} + \frac{3}{\sqrt{2}r_c}\hat{A}_2^{(0)}\mathrm{Pf.}\left(\eta\ln\frac{\eta-1}{\eta+1} - \frac{2}{\eta^2-1}\right)\right] \qquad \eta > 1, \tag{1.32}$$

again to $O(\mathrm{E}^{\frac{1}{2}})$. Note that the terms linear in η, at leading order and at $O(\mathrm{E}^{\frac{1}{2}})$, have been combined into a single term, $\hat{A}_1\eta$, in (1.31). While $\hat{A}_2^{(0)} = -\frac{\hat{u}_r(r_c;r_c)}{2}$, and $\hat{A}_{1\pm}^{(1)}$ in the above expressions are given by (1.26) and (1.28), respectively, $\hat{A}_1$ in (1.31) remains arbitrary. The prefix Pf. in (1.30)-(1.32) denotes a principal-finite-part interpretation (Gakhov 1990) which, as will be seen below, is required in interpreting the axial vorticity field within the elastic boundary layer. The expressions (1.30)-(1.32), taken together with the expressions for the constants involved, show that the CS-modes for small but finite E involve two parameters. These may be taken as $[\hat{u}_r(r_c;r_c) - r_c^{-(m+1)}]$ and $\hat{A}_1$, where $1/r_c^{m+1}$ is the normalized radial velocity associated with the Kelvin mode at $r = r_c$. The first parameter, of course, already exists for $\mathrm{E} = 0$, and is proportional to the amplitude of the second vortex sheet, $A(r_c)$, used earlier for the description of the CS-modes for $\mathrm{E} = 0$ (see (1.2)-(1.4)). The second parameter arises only for non-zero E and affects the detailed structure of the (elastic) boundary layer vorticity field.

The finite-E generalization of the regular Kelvin mode may be obtained by taking $r_c =$

r_{ck}, $c_1^{(0)}=0$, $c_2^{(0)}=1$, as for the inviscid case above. This implies $\hat{A}_2^{(0)}=-1/(2r_{ck}^{m+1})$, $\hat{A}_1^{(1-)}=\hat{A}_1^{(1+)}=-(2m+5)/(\sqrt{2}r_{ck}^{m+2})$. In the outer region, one now has $\hat{u}_{r1}(r;r_c)=\hat{u}_{r2}(r;r_c)=1/r^{m+1}$, and within the boundary layer, (1.30)-(1.32) take the form:

$$\tilde{u}_{rk-}(\eta)=-\frac{1}{2r_{ck}^{m+1}}\mathrm{Pf.}\eta\ln\frac{\eta-1}{\eta+1}-\frac{\mathrm{E}^{\frac{1}{2}}\eta}{\sqrt{2}r_{ck}^{m+2}}\left[(2m+5)+\frac{3}{2}\mathrm{Pf.}\left(\eta\ln\frac{\eta-1}{\eta+1}-\frac{2}{\eta^2-1}\right)\right]\quad \eta<-1, \tag{1.33}$$

$$\tilde{u}_{rk}(\eta)=\eta\left[\hat{A}_1-\frac{1}{2r_{ck}^{m+1}}\mathrm{Pf.}\ln\frac{1-\eta}{1+\eta}\right]-\frac{3E^{\frac{1}{2}}\eta}{2\sqrt{2}r_{ck}^{m+2}}\mathrm{Pf.}\left(\eta\ln\frac{1-\eta}{1+\eta}-\frac{2}{\eta^2-1}\right)\quad -1<\eta<-1, \tag{1.34}$$

$$\tilde{u}_{rk+}(\eta)=-\frac{1}{2r_{ck}^{m+1}}\mathrm{Pf.}\eta\ln\frac{\eta-1}{\eta+1}-\frac{\mathrm{E}^{\frac{1}{2}}\eta}{\sqrt{2}r_{ck}^{m+2}}\left[(2m+5)+\frac{3}{2}\mathrm{Pf.}\eta\left(\eta\ln\frac{\eta-1}{\eta+1}-\frac{2}{\eta^2-1}\right)\right]\quad \eta>1, \tag{1.35}$$

The above expressions suggest that the finite-E generalization of the regular Kelvin mode is a one-parameter family of singular eigenfunctions, $\hat{A}_1$ being the parameter, with singularities at $r=r_{ck}\pm\sqrt{2\mathrm{E}}\,(\eta=\pm1)$ for small E.

The above interpretation for finite E also becomes clear on consideration of the axial vorticity field associated with (1.30)-(1.32) (recall that the velocity field in the outer regions is irrotational to $O(\mathrm{E}^{\frac{1}{2}})$). For E = 0, the axial vorticity field is, of course, a delta function at $r=r_c$. For small but finite E, the vorticity field is still localized in the elastic boundary layer which may be regarded as a vortex sheet on the scale of the outer region. One may therefore discriminate between the 2D CS-modes and Kelvin mode based on the strength of this equivalent vortex sheet, defined as the total vorticity contained within the $O(\mathrm{E}^{\frac{1}{2}})$ boundary layer over a single wavelength in the azimuthal direction. For $\mathrm{E}\ll1$, this integrated vorticity contribution is proportional to $\int_{r_c-r\gg O(\mathrm{E}^{\frac{1}{2}})}^{r-r_c\gg O(\mathrm{E}^{\frac{1}{2}})}\hat{w}_z(r;r_c)rdr=(2\mathrm{E})^{\frac{1}{2}}\int_{-\infty}^{\infty}\tilde{w}_z(\eta)[r_c+(2\mathrm{E})^{\frac{1}{2}}\eta]d\eta$.

Using the relation $\hat{w}_z=(\mathrm{i}/m)\mathcal{L}(r\hat{u}_r)$, together with the small E expansion for the radial velocity in the boundary layer, one obtains $\tilde{w}_z(\eta)=(2\mathrm{E})^{-1}[\tilde{w}_z^{(0)}(\eta)+\mathrm{E}^{\frac{1}{2}}\tilde{w}_z^{(1)}(\eta)]$ where:

$$\tilde{w}_z^{(0)}(\eta)=\frac{\mathrm{i}r_c}{m}\frac{d^2\tilde{u}_r^{(0)}}{d\eta^2}, \tag{1.36}$$

$$=\frac{\mathrm{i}r_c}{m}\left[-\mathrm{Pf.}\frac{4\hat{A}_2^{(0)}}{(\eta^2-1)^2}+\hat{A}_1[\delta(\eta+1)-\delta(\eta-1)+\delta'(\eta+1)+\delta'(\eta-1)]\right], \tag{1.37}$$

$$\tilde{w}_z^{(1)}(\eta)=\frac{\mathrm{i}}{m}\left[\sqrt{2}\left(\eta\frac{d^2\tilde{u}_r^{(0)}}{d\eta^2}+3\frac{d\tilde{u}_r^{(0)}}{d\eta}\right)+r_c\frac{d^2\tilde{u}_r^{(1)}}{d\eta^2}\right], \tag{1.38}$$

$$=\mathcal{P}\frac{\mathrm{i}\hat{\mathrm{A}}_2^{(0)}}{m}\left[\sqrt{2}\left(\frac{2\eta(3\eta^2-5)}{(\eta^2-1)^2}+3\ln|\frac{\eta-1}{\eta+1}|\right)+2r_c\left(\ln|\frac{\eta-1}{\eta+1}|+\frac{2\eta(\eta^4-4\eta^2-1)}{(\eta^2-1)^3}\right)\right]$$
$$+\frac{\mathrm{i}r_c}{m}[\hat{A}_{1-}^{(1)}\{\delta'(\eta+1)-\delta(\eta+1)\}+\hat{A}_{1+}^{(1)}\{\delta'(\eta-1)+\delta'(\eta-1)\}], \tag{1.39}$$

where $\mathcal{P}$ denotes a Cauchy-principal-value interpretation. The integrated boundary-layer

vorticity, for small E, may be written as:

$$(2\mathrm{E})^{\frac{1}{2}}\int_{-\infty}^{\infty}\tilde{w}_z(\eta)[r_c+(2\mathrm{E})^{\frac{1}{2}}\eta]d\eta \tag{1.40}$$

$$=\frac{1}{(2\mathrm{E})^{\frac{1}{2}}}\left[r_c\int_{-\infty}^{\infty}\tilde{w}_z^{(0)}(\eta)d\eta+\mathrm{E}^{\frac{1}{2}}\left(\sqrt{2}\int_{-\infty}^{\infty}\tilde{w}_z^{(0)}(\eta)\eta d\eta+r_c\int_{-\infty}^{\infty}\tilde{w}_z^{(1)}(\eta)d\eta\right)\right], \tag{1.41}$$

$$=-\frac{4\mathrm{i}r_c^2}{m(2\mathrm{E})^{\frac{1}{2}}}\mathrm{Pf.}\int_{-\infty}^{\infty}\frac{d\eta}{(\eta^2-1)^2}+\frac{\mathrm{i}r_c}{m}(\hat{A}_{1+}^{(1)}-\hat{A}_{1-}^{(1)})+O(\mathrm{E}^{\frac{1}{2}}), \tag{1.42}$$

$$=\frac{\mathrm{i}r_c}{m}(\hat{A}_{1+}^{(1)}-\hat{A}_{1-}^{(1)})+O(\mathrm{E}^{\frac{1}{2}}), \tag{1.43}$$

where the Cauchy-principal-value interpretation implies that only the terms proportional to $\hat{A}_{1\pm}^{(1)}$ in (1.39) contribute. Physically, the contributions that are odd in η denote jet-like structures, either localized at the travelling wave singularities (proportional to $\delta'(\eta\pm1)$) or non-local, within the elastic boundary layer, and their contribution to the outer velocity field is negligibly small for $\mathrm{E}\ll1$. The second term in (1.42) is expected, and denotes the strength of the elastic boundary layer, interpreted as an equivalent vortex sheet, on the outer scale. This vortex-sheet contribution is present only for the CS-modes, and vanishes for the Kelvin mode in which case $\hat{A}_{1+}^{(1)}=\hat{A}_{1-}^{(1)}$. The first term in (1.42) is larger, being $O(\mathrm{E}^{-\frac{1}{2}})$, but does not contribute to the outer velocity field owing to the principal finite-part interpretation. Thus, the vortex-sheet contribution, proportional to $\hat{A}_{1+}^{(1)}-\hat{A}_{1-}^{(1)}$, is the only relevant one as far as the induced velocity field in the outer region is concerned, ensuring consistency with the inviscid scenario in the limit $\mathrm{E}\to0$. In terms of the vorticity field in the elastic boundary layer requiring a principal-finite-part interpretation, the relation between the finite E CS-modes, and those for $\mathrm{E}=0$, is similar to that between the three-dimensional CS-modes of a smooth vorticity profile and those of a Rankine vortex (Roy & Subramanian (2014*b*)).

Having established in detail a connection between the solutions of the elastic Rayleigh equation for small but finite E, and the original inviscid spectrum of the Rankine vortex (including the Kelvin mode), we proceed towards an alternate intepretation of the CS-eigenfunctions for non-zero E. As will be seen, this interpretation is more general in that it is not reliant on E being small. The presence of two parameters, $\hat{u}_r(r_c;r_c)-1/r_c^{m+1}$ and $\hat{A}_1$ in (1.29)-(1.32), implies the existence of a pair of continuous spectra for finite E, in contrast to the single one for $\mathrm{E}=0$. It is convenient to regard each of these as corresponding to a particular choice of $\hat{A}_1$ in (1.31), and therefore, as being parameterized by $\hat{u}_r(r_c;r_c)-1/r_c^{m+1}$ alone. The natural choices are $\hat{A}_1=\mathrm{E}^{\frac{1}{2}}\hat{A}_{1+}^{(1)}$ and $\hat{A}_1=\mathrm{E}^{\frac{1}{2}}\hat{A}_{1-}^{(1)}$ which ensure the smooth connection of the regular solution across $\eta=1$ and -1, respectively. For either choice, the absence of a kink ensures the absence of delta-function-like contributions to the tangential velocity and axial vorticity fields at the relevant travelling wave singularity. Of course, the finite-E eigenfunction is still singular owing to the logarithmic terms in (1.30)-(1.32). From here onwards, the singularities at $\eta=1$ and -1 will be associated with the fast (or forward) and slow (or backward) shear wave, respectively, for obvious reasons. The choice $\hat{A}_1=\hat{A}_{1+}^{(1)}$ implies that one only has a kink at the slow shear wave. Since it is this kink that allows for singular eigenfunctions even as r_c spans a continuous interval, the interval of existence for this slow-shear-wave-spectrum (SSWS) may be obtained by the requirement that the kink (the location of the slow shear wave singularity) lie in the physical domain. The slow shear wave propagates with an angular frequency of $\omega=m[\Omega(r)+\Omega'(r)(2\mathrm{E})^{\frac{1}{2}}]=m[1/r^2-2(2\mathrm{E})^{\frac{1}{2}}/r^3]$, which must then lie in

the base-state range of angular frequencies $(0, m)$. The shear wave frequency evidently approaches zero for $r \to \infty$, while it equals m for $r = r_{cs}$ with $1/r_{cs}^2 - 2(\mathrm{E})^{\frac{1}{2}}/r_{cs}^3 = 1$. For small E this gives $r_{cs} = 1 - (2\mathrm{E})^{\frac{1}{2}}$, corresponding to an angular frequency of $1 + 2(2\mathrm{E})^{\frac{1}{2}}$. So, the SSWS frequency interval is $[0, m(1 + 2(2\mathrm{E})^{\frac{1}{2}})]$. Analogous arguments for the fast shear wave yield the frequency interval for the fast-shear-wave-spectrum (FSWS) as $[0, m(1 - 2(2\mathrm{E})^{\frac{1}{2}})]$ for small E. The SSWS and FSWS eigenfunctions differ in structure only within the $O(\mathrm{E}^{\frac{1}{2}})$ boundary layer, where they are given by

$$\tilde{u}_{r-}(\eta) = \hat{A}_2^{(0)}\mathrm{Pf.}\eta \ln\frac{\eta-1}{\eta+1} + \mathrm{E}^{\frac{1}{2}}\eta\left[\hat{A}_{1-}^{(1)} + \frac{3}{\sqrt{2}r_c}\hat{A}_2^{(0)}\mathrm{Pf.}\left(\eta\ln|\frac{\eta-1}{\eta+1}| - \frac{2}{\eta^2-1}\right)\right] \quad \eta < -1, \quad (1.44)$$

$$\tilde{u}_{r+}(\eta) = \hat{A}_2^{(0)}\mathrm{Pf.}\eta \ln|\frac{\eta-1}{\eta+1}| + \mathrm{E}^{\frac{1}{2}}\eta\left[\hat{A}_{1+}^{(1)} + \frac{3}{\sqrt{2}r_c}\hat{A}_2^{(0)}\mathrm{Pf.}\left(\eta\ln\frac{\eta-1}{\eta+1} - \frac{2}{\eta^2-1}\right)\right] \quad \eta > -1, \quad (1.45)$$

and

$$\tilde{u}_{r-}(\eta) = \hat{A}_2^{(0)}\mathrm{Pf.}\eta \ln|\frac{\eta-1}{\eta+1}| + \mathrm{E}^{\frac{1}{2}}\eta\left[\hat{A}_{1-}^{(1)} + \frac{3}{\sqrt{2}r_c}\hat{A}_2^{(0)}\mathrm{Pf.}\left(\eta\ln|\frac{\eta-1}{\eta+1}| - \frac{2}{\eta^2-1}\right)\right] \quad \eta < 1, \quad (1.46)$$

$$\tilde{u}_{r+}(\eta) = \hat{A}_2^{(0)}\mathrm{Pf.}\eta \ln\frac{\eta-1}{\eta+1} + \mathrm{E}^{\frac{1}{2}}\eta\left[\hat{A}_{1+}^{(1)} + \frac{3}{\sqrt{2}r_c}\hat{A}_2^{(0)}\mathrm{Pf.}\left(\eta\ln\frac{\eta-1}{\eta+1} - \frac{2}{\eta^2-1}\right)\right] \quad \eta > 1, \quad (1.47)$$

respectively, to $\mathrm{O}(\mathrm{E}^{\frac{1}{2}})$. The SSWS interval above extends outside the base-state interval of angular frequencies, clearly implying that the modified semi-circle theorem stated earlier doesn't apply to the CS-modes. The equivalence of the CS-interval to the semi-circle radius, for the purely inviscid case, is thus a coincidence. It is worth noting that the expressions (1.44)-(1.47) are valid only when the elastic boundary layer is at a distance away from the core that is much greater than $\mathrm{O}(\sqrt{\mathrm{E}})$. Strictly speaking, derivation of the finite-E eigenfunctions for frequencies close to the upper end of the SSWS and FSWS intervals requires application of the core boundary condition to a uniformly valid representation constructed from both the outer and boundary layer solutions. This is a detail, however, and can be done (Reddy (2015)).

The point that needs emphasis, with regard to the alternate interpretation above, is its validity for arbitrary E. Although closed form expressions for the eigenfunctions, belonging to the two continuous spectra, can no longer be obtained when E is not small, the pair of travelling wave singularities still exist and satisfy $\omega = m[\Omega(r) \pm 2\Omega'(r)(2\mathrm{E})^{\frac{1}{2}}]$. The elastic boundary layer solution given in (1.15) must now be interpreted as a Frobenius expansion in the vicinity of the relevant singular point. The FSWS spectrum corresponds to the interval $[0, m(1 - 2(2\mathrm{E})^{\frac{1}{2}})]$ for $\mathrm{E} < 1/8$, and to $[m(1 - 2(2\mathrm{E})^{\frac{1}{2}}), 0]$ for $\mathrm{E} > 1/8$. The SSWS spectrum continues to be given by $[0, m(1 + 2(2\mathrm{E})^{\frac{1}{2}})]$ for finite E, although there arises a degeneracy for $\mathrm{E} > 1/18$ due to shear waves at a pair of radial locations propagating with the same frequency. Figures 1 and 2 show the spectra, and a few representative eigenfunctions, for the hyperbolic tangent vorticity profile defined as,

$$Z(r) = \frac{Z_0}{2}\left\{1 - \tanh\left[\frac{r-a}{d}\right]\right\}, \quad (1.48)$$

determined numerically using a spectral method (cf. section 3 in the main text). Figure 3 shows a comparison between the numerical and analytical estimates for the upper (and lower) bounds of the SSWS (and FSWS) intervals with E for this vorticity profile.

The close analogy of the Rankine vortex with plane Couette flow (Roy & Subramanian (2014*b*)) allows one to identify the travelling-wave spectra in the latter case too. For the

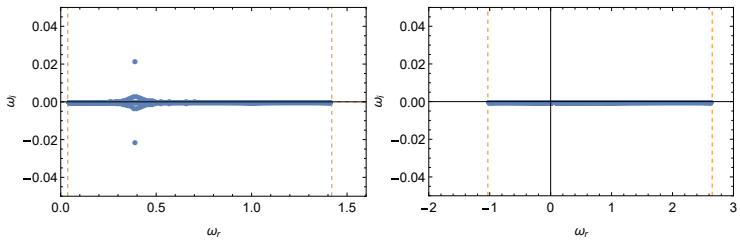

(a) (b)

Figure 1: The elastic Rayleigh spectrum for the hyperbolic tangent vorticity profile (defined in (1.48)) with $d = 0.025$ for (a) E = 0.1 and (b) E = 1; $m = 2$ and $N = 1500$. In addition to the continuous spectrum, we see a pair of discrete modes for E = 0.1. For the numerical calculation, the domain chosen is $r \in (0, r_\infty)$ with $r_\infty = 4a$. Hence the continuous spectrum eigenvalues lie between ω_{min} and ω_{max} which can be found analytically, using the expressions derived in the main text, and are marked on the plot.

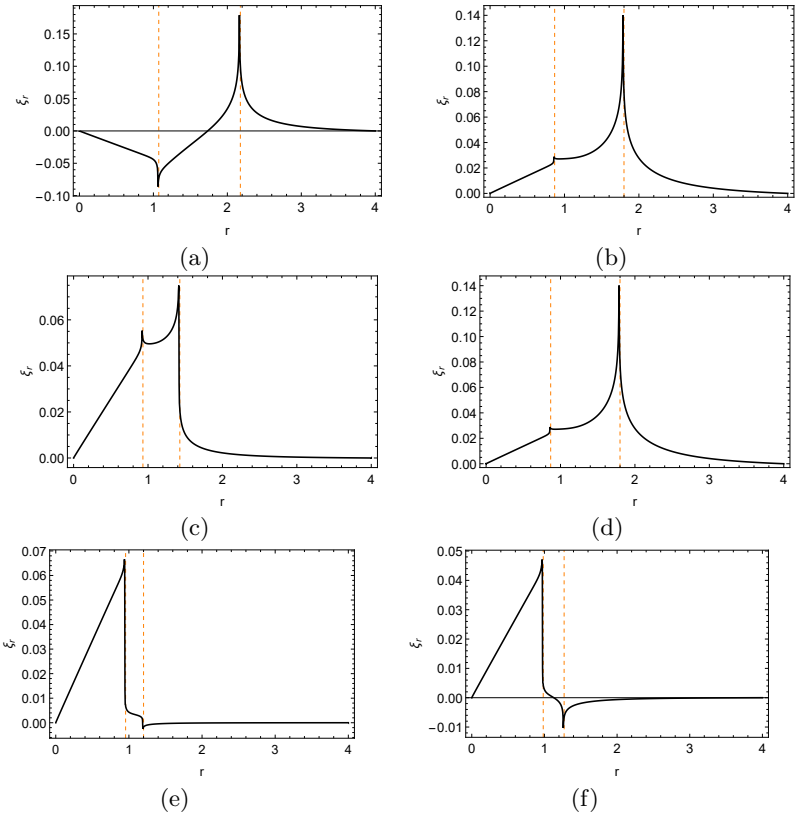

Figure 2: The radial displacement eigenfunctions for the CS-modes associated with the hyperbolic tangent vorticity profile (defined in (1.48)); E = $0.1, m = 2$ for (a), (c), (e); E = $1, m = 2$ for (b), (d), (f). The wavespeeds are given by, ω_r = (a) 0.3, (c) 0.8 and (e) 1.2 for E = 0.1 and by ω_r = (b) -0.7, (d) 0.8 and (f) 2 for E = 1. The analytical locations for the shear-wave singularities are marked as red (dashed) lines.

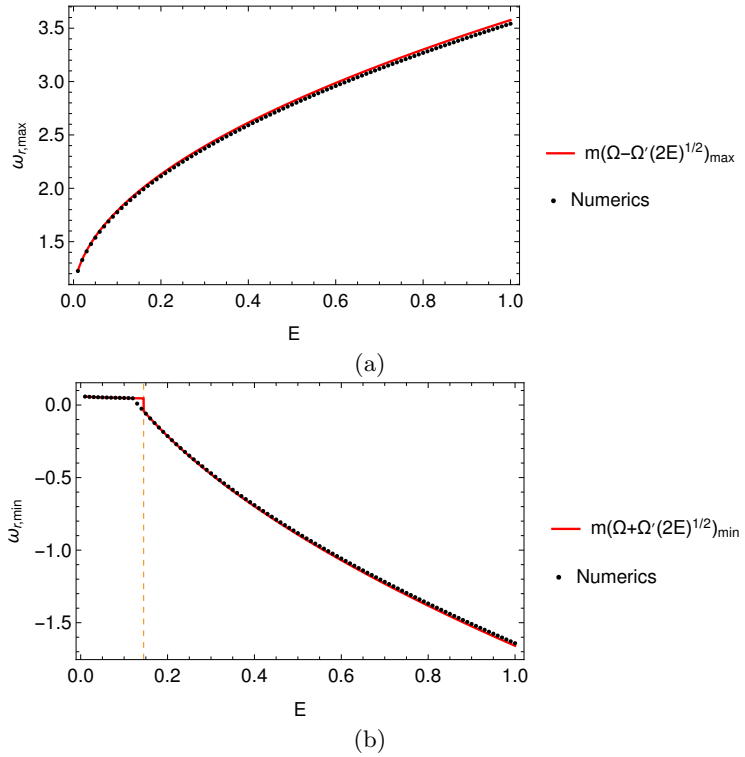

Figure 3: Variation of the global (a) upper and (b) lower bounds of the continuous spectrum with E, for the hyperbolic tangent vorticity profile (defined in (1.48)) with $d = 0.025$. For SSWS, the lower bound is 0 while the upper bound is shown in (a). On the other hand for the FSWS, for $\mathrm{E} < 0.145$, the lower bound is 0 while the upper bound is shown in (b). For FSWS, for $\mathrm{E} > 0.145$, the lower bound is shown in (b) while the upper bound is 0. In (b), the threshold $\mathrm{E} \sim 0.145$ is marked. Note that due to the bounded domain the transition threshold for FSWS is different from that for an unbounded vortex ($\mathrm{E} = 1/8$).

(dimensionless) base-state profile $U(y) = y$ in the domain $(0, 1)$, the FSWS and SSWS span the intervals $[-(2\mathrm{E})^{\frac{1}{2}}, 1-(2\mathrm{E})^{\frac{1}{2}}]$ and $[(2\mathrm{E})^{\frac{1}{2}}, 1+(2\mathrm{E})^{\frac{1}{2}}]$, both of which violate the semi-circle theorem. Unlike the Rankine vortex, the linearity of the Couette profile implies that the aforementioned spectral intervals remain valid for arbitrary E, and become disjoint for $\mathrm{E} > 1/8$. An analysis similar to that detailed above, but simpler, can be carried out for plane Couette flow to obtain expressions for the singular eigenfunctions corresponding to the fast and slow shear wave spectra in the limit $\mathrm{E} \ll 1$. The outer solutions, valid when $|y - y_c| \gg \mathrm{E}^{\frac{1}{2}}$ with y_c being the critical level, are the well-known Case eigenfunctions with the normal velocity given by $\hat{u}_y(y; y_c) = \sinh k(1 - y_c) \sinh ky$ for $0 < y < y_c$ and $\hat{u}_y(y; y_c) = \sinh ky_c \sinh k(1-y)$ for $y < y_c < 1$ (Case (1960)). Within the elastic boundary layer, the SSWS eigenfunctions are given by:

$$\tilde{u}_{y-}(\eta) = \hat{B}_2 \mathrm{Pf}.\eta \ln\frac{\eta-1}{\eta+1} + (2\mathrm{E})^{\frac{1}{2}}\eta\hat{B}_{1-} \quad \eta < -1, \tag{1.49}$$

$$\tilde{u}_{y+}(\eta) = \hat{B}_2 \mathrm{Pf}.\eta \ln\left|\frac{\eta-1}{\eta+1}\right| + (2\mathrm{E})^{\frac{1}{2}}\eta\hat{B}_{1+} \quad \eta > -1, \tag{1.50}$$

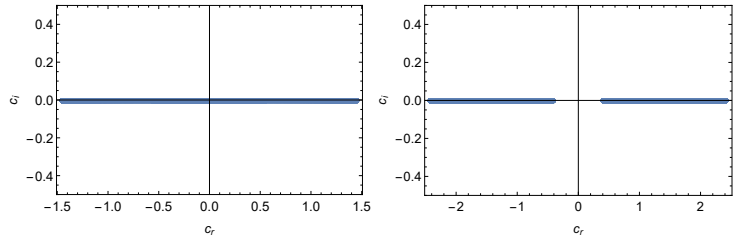

(a) (b)

Figure 4: The elastic Rayleigh spectrum for plane Couette flow for (a) E = 0.1 and (b) E = 1; $k = 2$ and $N = 1500$.

and the FSWS eigenfunctions are given by:

$$\tilde{u}_{y-}(\eta) = \hat{B}_2 \mathrm{Pf.} \eta \ln\left|\frac{\eta-1}{\eta+1}\right| + (2\mathrm{E})^{\frac{1}{2}} \eta \hat{B}_{1-} \quad \eta < 1, \tag{1.51}$$

$$\tilde{u}_{y+}(\eta) = \hat{B}_2 \mathrm{Pf.} \eta \ln\frac{\eta-1}{\eta+1} + (2\mathrm{E})^{\frac{1}{2}} \eta \hat{B}_{1+} \quad \eta > 1, \tag{1.52}$$

Here, $\eta = (y - y_c)/(2\mathrm{E})^{\frac{1}{2}}$ is the boundary layer variable, and the constants appearing in (1.49)-(1.52) are $\hat{B}_2 = -\frac{1}{2}\hat{u}_y(y_c; y_c)$ with $\hat{u}_y(y_c; y_c) = \sinh ky_c \sinh k(1 - y_c)$ being the normal velocity at the critical level, and $\hat{B}_{1+} = -k \cosh k(1 - y_c) \sinh ky_c$ and $\hat{B}_{1-} = k \cosh ky_c \sinh k(1 - y_c)$. Since the original inviscid spectrum is purely continuous, the exceptional case of $\hat{B}_{1+} = \hat{B}_{1-}$, corresponding to the Kelvin mode for the Rankine vortex above, does not arise. Figures 4 and 5 show the spectra, and a few representative eigenfunctions, for plane Couette flow for E's on either side of the overlap threshold (E = 1/8), again determined using a spectral method (cf. next section).

The CS-modes arising from the multiple continuous spectra above, together with a possibly finite number of discrete modes, must form a complete basis for the independent fields required to completely characterize an initial state in the limit $Re, De \to \infty$. For the Rankine vortex, as governed by the elastic Rayleigh equation, these may be taken as the radial velocity field and the two components of the polymeric force field, $\nabla \cdot \boldsymbol{a}$; since the radial component of the normal stress, a_{rr}, does not enter in the elastic Rayleigh limit, one may equivalently consider the radial velocity field and the stress components $a_{r\theta}$ and $a_{\theta\theta}$. One therefore needs (at least) three continuous spectra in order to represent an arbitrary initial condition. The analysis detailed above, in choosing a continuous solution across $r = r_c\,(\eta = 0)$, does not account for the third spectrum needed. This is the Doppler spectrum corresponding to $\omega = \Omega(r_c)$. Now, the Frobenius exponents for $r = r_c$, for the radial displacement field, are 0 and 1, and there is no singularity at $r = r_c\,(\eta = 0)$, as is also evident from the elastic boundary layer solutions above (see (1.15) above). However, in a manner similar to inviscid plane Couette flow (Case (1960)), one nevertheless requires CS-modes with a singularity at $r = r_c$ to generate a complete basis. The Doppler spectrum eigenfunctions, for finite E, with $De \to \infty$, may be generated by different choices of one of the two regular solutions on either side of $r = r_c$ (the one corresponding to a Frobenius exponent of 0). On including the effects of relaxation, $r = r_c$ becomes a singular point. The functional form of the CS-modes has been obtained earlier (Graham (1998)). For large but finite De, these modes, arising from the solution of a fourth-order ODE, will be valid in an inner layer of $O(De^{-1})$ (with $De^{-1} \ll \sqrt{\mathrm{E}}$), and

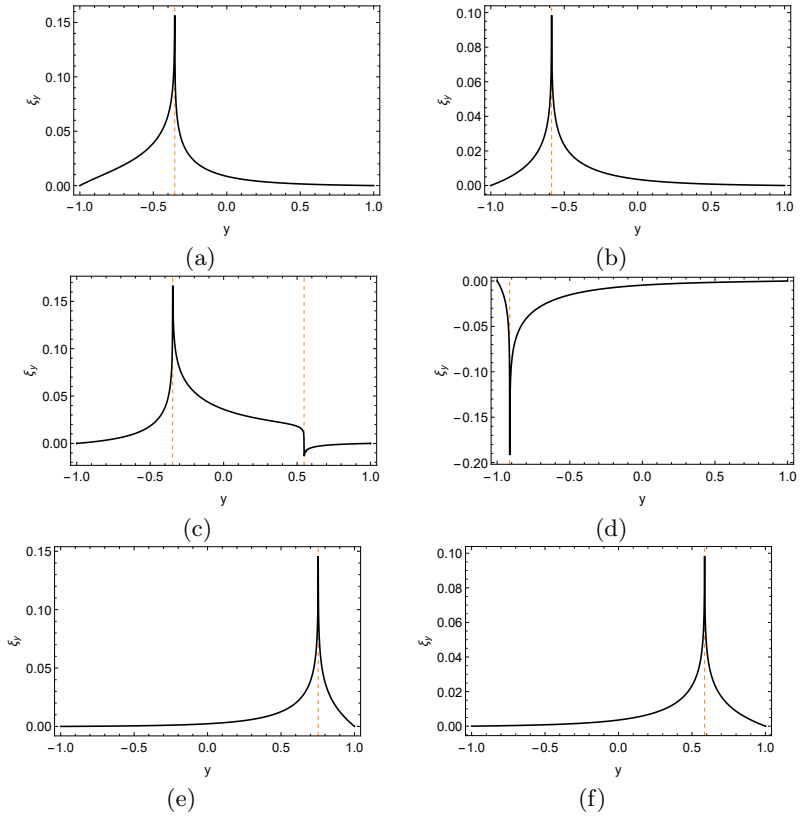

Figure 5: The wall-normal displacement eigenfunctions for plane Couette flow for the CS-modes; $\mathrm{E} = 0.1, k = 2$ for (a), (c), (e); $\mathrm{E} = 1, k = 2$ for (b), (d), (f). The wavespeeds are given by $c_r =$ (a) -0.8, (c) 0.1 and (e) 1.2 for $\mathrm{E} = 0.1$ and by $c_r =$ (b) -2, (d) 0.5 and (f) 2 for $\mathrm{E} = 1$. The analytical locations for the fast and/or slow travelling-wave singularities are marked as red (dashed) lines.

will transition to the elastic Rayleigh Doppler-spectrum eigenfunctions on scales much larger than $O(De^{-1})$.

2. Details of the analysis for the LHS problem

The approach used in section 3.2 of the main text, may be validated by the exactly soluble LHS problem - that governed solely by the LHS of (3.2) of the main text for the Rankine profile. The governing equation for the LHS problem is:

$$D\left[r^3\left\{(\omega - m\Omega)^2 - 2m^2\mathrm{E}\Omega'^2\right\}D\xi\right] = 0 \tag{2.1}$$

with $\Omega = 1/r^2$, $\Omega' = -2/r^3$ and the boundary conditions:

$$\xi\Big|_{r=1} = 1, \tag{2.2}$$

$$\frac{d\xi}{dr}\Big|_{r=1+} = \frac{(m-1)(\omega - m)^2}{(\omega - m)^2 - 8m^2\mathrm{E}}, \tag{2.3}$$

$$\xi \to 0, \qquad \text{as } r \to \infty. \tag{2.4}$$

As will be seen below, the eigenvalue expression obtained from the LHS problem agrees with the complete problem to $\mathrm{O}(g\sqrt{\mathrm{E}})$.

The solution of (2.1) may be readily written as,

$$\xi = \frac{\displaystyle\int_r^\infty \frac{dr'}{r'^3 P(r')}}{\displaystyle\int_1^\infty \frac{dr'}{r'^3 P(r')}}, \tag{2.5}$$

where $P(r) = (\omega - m\Omega(r))^2 - 2m^2\mathrm{E}\Omega'(r)^2$, defined in the main text. (2.5) satisfies the first and third boundary conditions above by construction. Applying the remaining boundary condition (2.3), leads to the following dispersion relation, valid for arbitrary E:

$$\mathcal{D}(\omega, m; \mathrm{E}) \equiv 1 + (m-1)(\omega - m)^2 \int_1^\infty \frac{dr'}{r'^3 P(r')} = 0 \tag{2.6}$$

A Nyquist method, following Balmforth (1998), can be used establish the presence of an unstable mode (not shown).

2.1. *Small-E expansion of the exact solution*

Next, we analyze (2.6) to obtain the scaling for the growth rate in the limit of small E. (2.6), explicitly written out after evaluation of the integral in closed form, takes the form

$$\begin{aligned}\mathcal{D}(\omega, m; \mathrm{E}) \equiv 1 + \frac{(m-1)f^2}{(\eta_1-\eta_2)(\eta_2-\eta_3)(\eta_3-\eta_1)} \{&\eta_1(\eta_2-\eta_3)\log(1-\eta_1) + \eta_2(\eta_3-\eta_1)\log(1-\eta_2) + \\ &\eta_3(\eta_1-\eta_2)\log(1-\eta_3)\} = 0,\end{aligned} \tag{2.7}$$

where $f = m/\omega - 1$ and $\eta_{1,2,3}$ are the roots of the cubic: $\eta(\eta - 1 - f)^2 - 8(1+f)^2\mathrm{E} = 0$. The exact expressions for $\eta_{1,2,3}$ are omitted for brevity. We make the *a priori* assumption of $f \ll 1$ but do not specify its smallness relative to E; implying that the unstable mode exists in the vicinity of the core. As already argued in section **??**, this is a reasonable assumption since the balance between elastic and inertial terms in P occurs when $\omega - m \sim O(\sqrt{\mathrm{E}})$. Expanding the exact expressions of $\eta_{1,2,3}$ for small values of E and f, one obtains,

$$\begin{aligned}\eta_1 = 1 + 2\sqrt{2\mathrm{E}} - 4\mathrm{E} + 10\sqrt{2}\mathrm{E}^{3/2} - 64\mathrm{E}^2 + f\left(1 + \sqrt{2\mathrm{E}} - 5\sqrt{2}\mathrm{E}^{3/2} + 64\mathrm{E}^2 + \ldots\right) \\ + f^2\left(-\frac{\sqrt{\mathrm{E}}}{2\sqrt{2}} + \frac{15\mathrm{E}^{3/2}}{2\sqrt{2}} - 64\mathrm{E}^2 + \ldots\right) + \ldots,\end{aligned} \tag{2.8}$$

$$\eta_2 = 8\mathrm{E} + 128\mathrm{E}^2 - 128f\mathrm{E}^2 + 128f^2\mathrm{E}^2 + \ldots, \tag{2.9}$$

$$\begin{aligned}\eta_3 = 1 - 2\sqrt{2\mathrm{E}} - 4\mathrm{E} - 10\sqrt{2}\mathrm{E}^{3/2} - 64\mathrm{E}^2 + f\left(1 - \sqrt{2\mathrm{E}} + 5\sqrt{2}\mathrm{E}^{3/2} + 64\mathrm{E}^2 + \ldots\right) \\ + f^2\left(\frac{\sqrt{\mathrm{E}}}{2\sqrt{2}} - \frac{15\mathrm{E}^{3/2}}{2\sqrt{2}} - 64\mathrm{E}^2 + \ldots\right) + \ldots\end{aligned} \tag{2.10}$$

Substituting the above expansions in (2.7), again expanding for small E, yields the asymptotic expansion for f. The corresponding expression for ω is found to be,

$$\frac{\omega}{m} \sim 1 - \sqrt{\mathrm{E}}\left[\sqrt{8} + e^{-\frac{1}{m-1}\left(\sqrt{\frac{2}{\mathrm{E}}}-6\right)}\left\{2\sqrt{8} - 16\sqrt{\mathrm{E}} + 4\sqrt{8}\mathrm{E} - 128\mathrm{E}^{3/2}\log(32\mathrm{E}) - 64(3+4i\pi)\mathrm{E}^{3/2}\right\}\right] \tag{2.11}$$

It is evident that $f = m/\omega - 1 \sim O(\sqrt{\mathrm{E}}) \ll 1$, ensuring self-consistency. The above expression highlights the transcendentally small nature of the growth rate; specifically $\omega_i = 256\pi \mathrm{E}^2 e^{-\frac{1}{m-1}\left(\sqrt{\frac{2}{\mathrm{E}}}-6\right)}$ in the limit $E \ll 1$. Note that in contrast to the growth rate, the correction to the leading order wave speed has an algebraic scaling, $1-\omega_r \sim O(\sqrt{\mathrm{E}})$, consistent with the initial scaling arguments in section 3.2 of the main text.

2.2. *Matched Asymptotics Expansions approach*

Here we give the details for the solution of the LHS problem using using the matched asymptotics expansions approach. The answer obtained to $O(\mathrm{E}^2 e^{-\frac{1}{m-1}\sqrt{\frac{2}{\mathrm{E}}}})$ matches exactly with that obtained from the exact solution (2.11 above). This serves to validate use of the technique for the full problem for which an exact solution is not available. We assume the following double expansion for the eigenvalue for $E \ll 1$ and $g \ll 1$:

$$\frac{\omega}{m} = 1 - \sqrt{\mathrm{E}}\left[\sqrt{8} + g\left\{c_0 + c_1\sqrt{\mathrm{E}} + c_2\mathrm{E} + \ldots\right\} + O(g^2)\right] \tag{2.12}$$

As will be seen, the transcendental scaling for g naturally emerges in this approach, implying that (2.12) conforms to the exponential asymptotics ansatz; the transcendentally small terms of $\mathrm{O}(g)$ in this expansion are important since they determine the growth rate at leading order. The boundary layer structure is the same as that of the full problem, and has been discussed in detail in the main text.

2.2.1. *Outer region- $r - 1 \sim O(1)$*

One expands P for small E as,

$$\frac{P}{m^2} = \mathcal{S}_0 + \sqrt{\mathrm{E}}\mathcal{S}_1 + \mathrm{E}\mathcal{S}_2 + \mathrm{O}(g\sqrt{\mathrm{E}}), \tag{2.13}$$

where $\mathcal{S}_0 = \left(1 - \frac{1}{r^2}\right)^2$, $\mathcal{S}_1 = -2\sqrt{8}\left(1 - \frac{1}{r^2}\right)$ and $\mathcal{S}_2 = 8\left(1 - \frac{1}{r^6}\right)$. This implies an expansion for the radial displacement of the form,

$$\xi^F(r) = \mathrm{E}\,\xi_0^F(r) + \mathrm{E}^{3/2}\,\xi_1^F(r) + \mathrm{E}^2\,\xi_2^F(r) + \mathrm{O}(\mathrm{E}^{5/2}) + \mathrm{O}(g\sqrt{\mathrm{E}}). \tag{2.14}$$

From section 3.1, we see that the RHS of (**??**) enters at all orders in the outer region. Thus, the outer region solutions of the full problem and LHS problem differ at all orders. For the LHS problem, at O(E),

$$\frac{d}{dr}\left[r^3 S_0 \frac{d\xi_0^F}{dr}\right] = 0 \tag{2.15}$$

with $\xi_0^F \to 0$ for $r \to \infty$, which gives $\xi_0^F(r) = \dfrac{\mathcal{B}_0}{(r^2-1)}$.

At $\mathrm{O}(\mathrm{E}^{3/2})$,

$$\frac{d}{dr}\left[r^3 S_0 \frac{d\xi_1^F}{dr}\right] = -\frac{d}{dr}\left[r^3 S_1 \frac{d\xi_0^F}{dr}\right], \tag{2.16}$$

with $\xi_1^F \to 0$ for $r \to \infty$, which gives $\xi_1^F(r) = \dfrac{2\sqrt{2}\mathcal{B}_0}{(r^2-1)^2} + \dfrac{4\sqrt{2}\mathcal{B}_0 + \mathcal{B}_1}{(r^2-1)}$.

At $\mathrm{O}(\mathrm{E}^2)$,

$$\frac{d}{dr}\left[r^3 S_0 \frac{d\xi_2^F}{dr}\right] = -\frac{d}{dr}\left[r^3 S_1 \frac{d\xi_1^F}{dr}\right] - \frac{d}{dr}\left[r^3 S_2 \frac{d\xi_0^F}{dr}\right], \tag{2.17}$$

with $\xi_2^F \to 0$ for $r \to \infty$, which gives, $\xi_2^F(r) = \dfrac{32\mathcal{B}_0}{3(r^2-1)^3} + \dfrac{20\mathcal{B}_0 + 2\sqrt{2}2\mathcal{B}_1}{(r^2-1)^2} + \dfrac{32\mathcal{B}_0 + 4\sqrt{2}\mathcal{B}_1 + \mathcal{B}_2}{(r^2-1)} +$

$8\mathcal{B}_0 \log \dfrac{r^2-1}{r^2}$. The $\mathcal{B}_i$'s in the above expressions are integration constants, which are determined by matching to the outer boundary-layer solution.

2.2.2. *Outer boundary layer - $r-1 \sim \sqrt{E}$*

In terms of the rescaled coordinate $x = (r-1)/\sqrt{\mathrm{E}}$, the LHS problem in the outer boundary layer takes the form:

$$\frac{d}{dx}\left[\mathcal{Q}\frac{d\xi^o}{dx}\right] = 0, \tag{2.18}$$

where $\mathcal{Q}$, for small E, is expanded as,

$$\mathcal{Q} = \mathcal{Q}_0 + \sqrt{\mathrm{E}}\mathcal{Q}_1 + \mathrm{E}\mathcal{Q}_2 + \mathrm{E}^{3/2}\mathcal{Q}_3 + \mathrm{O}(\mathrm{E}^2) + \mathrm{O}(g\sqrt{\mathrm{E}}), \tag{2.19}$$

with $\mathcal{Q}_0 = 4x(x-2\sqrt{2})$, $\mathcal{Q}_1 = -12\sqrt{2}x(x-2\sqrt{2})$, $\mathcal{Q}_2 = x^2(x^2-4\sqrt{2}x-24)$ and $\mathcal{Q}_3 = x^3(88-x^2)$. For the displacement, we assume the expansion,

$$\begin{aligned}\xi^o(x) = \sqrt{\mathrm{E}}\,\xi_0^o(x) + \mathrm{E}\,\xi_1^o(x) + \mathrm{E}^{3/2}\,\xi_2^o(x) + \\ \mathrm{E}^2\log(32\mathrm{E})\,\xi_{31}^o(x) + \mathrm{E}^2\,\xi_3^o(x) + \mathrm{O}(\mathrm{E}^{5/2}) + \mathrm{O}(g\sqrt{\mathrm{E}}).\end{aligned} \tag{2.20}$$

The log(32E) term in (2.20) is necessitated by the log term in the outer region solution at E^2 viz. ξ_2^F.

At $\mathrm{O}(\mathrm{E}^{1/2})$,

$$\frac{d}{dx}\left[\mathcal{Q}_0\frac{d\xi_0^o}{dx}\right] = 0 \tag{2.21}$$

$$\Rightarrow\ \xi_0^o(x) = \mathcal{G}_{10} + \mathcal{G}_{11}\log\left(\frac{x-2\sqrt{2}}{x}\right). \tag{2.22}$$

At O(E),

$$\frac{d}{dx}\left[\mathcal{Q}_0\frac{d\xi_1^o}{dx}\right] = -\frac{d}{dx}\left[\mathcal{Q}_1\frac{d\xi_0^o}{dx}\right], \tag{2.23}$$

$$\Rightarrow\ \xi_1^o(x) = \mathcal{G}_{21} + \mathcal{G}_{11}\log\left(\frac{x-2\sqrt{2}}{x}\right). \tag{2.24}$$

Note that at both $\mathrm{O}(\mathrm{E}^{1/2})$ and O(E) one obtains the same governing equation since $\mathcal{Q}_0$ and $\mathcal{Q}_1$ have an identical dependence on x (to within a multiplicative constant). At $\mathrm{O}(\mathrm{E}^{3/2})$,

$$\frac{d}{dx}\left[\mathcal{Q}_0\frac{d\xi_2^o}{dx}\right] = -\frac{d}{dx}\left[\mathcal{Q}_1\frac{d\xi_1^o}{dx}\right] - \frac{d}{dx}\left[\mathcal{Q}_2\frac{d\xi_0^o}{dx}\right], \tag{2.25}$$

$$\Rightarrow\ \xi_2^o(x) = \mathcal{G}_{22} + \mathcal{G}_{12}\log\left(\frac{x-2\sqrt{2}}{x}\right) - \frac{\mathcal{G}_{10}}{\sqrt{2}}\left(\frac{32}{x-2\sqrt{2}} + x - 2\sqrt{2}\right). \tag{2.26}$$

At $\mathrm{O}(\mathrm{E}^2\log(32\mathrm{E}))$,

$$\frac{d}{dx}\left[\mathcal{Q}_0\frac{d\xi_{31}^o}{dx}\right] = 0, \tag{2.27}$$

$$\Rightarrow\ \xi_{31}^o(x) = \tilde{\mathcal{G}}_{23} + \tilde{\mathcal{G}}_{13}\log\left(\frac{x-2\sqrt{2}}{x}\right). \tag{2.28}$$

At $\mathrm{O}(\mathrm{E}^2)$,

$$\frac{d}{dx}\left[\mathcal{Q}_0\frac{d\xi_3^o}{dx}\right] = -\frac{d}{dx}\left[\mathcal{Q}_1\frac{d\xi_2^o}{dx} + \mathcal{Q}_2\frac{d\xi_1^o}{dx} + \mathcal{Q}_3\frac{d\xi_0^o}{dx}\right] \tag{2.29}$$

$$\begin{aligned}\Rightarrow\ \xi_3^o(x) = {}& \mathcal{G}_{23} + \mathcal{G}_{13}\log\left(\frac{x-2\sqrt{2}}{x}\right) + 3\sqrt{2}\mathcal{G}_{12}\log\left(\frac{x-2\sqrt{2}}{x}\right)\\ & - 3\mathcal{G}_{10}\left(x + \frac{32}{x-2\sqrt{2}}\right) - \frac{\mathcal{G}_{11}}{\sqrt{2}}\left(\frac{32}{x-2\sqrt{2}} + x - 2\sqrt{2}\right)\\ & + \frac{\mathcal{G}_{10}}{\sqrt{2}}\left(\frac{(x-2\sqrt{2})^2}{2} + 6\sqrt{2}\left(x-2\sqrt{2}\right) - 64\log\left(x-2\sqrt{2}\right) + \frac{160\sqrt{2}}{x-2\sqrt{2}}\right).\end{aligned} \tag{2.30}$$

The $\mathcal{G}_{ij}$'s in the above expressions are integration constants, which are determined by matching to the far-field and inner boundary-layer solutions.

2.2.3. *Inner boundary layer - $r-1 \sim O(g\sqrt{E})$*

Introducing the inner boundary layer coordinate, $y = (r-1)/g\sqrt{\mathrm{E}}$ with $g, \mathrm{E} \ll 1$ and the inner boundary layer displacement as $\xi(r) = \xi^i(y)$, we have:

$$\frac{d}{dy}\left[\mathcal{R}\frac{d\xi^i}{dy}\right] = \frac{g^2\mathrm{E}\mathcal{R}(m^2-1)}{(1+g\sqrt{\mathrm{E}}y)^2}\xi^i, \tag{2.31}$$

with $\mathcal{R} = (1+g\sqrt{\mathrm{E}}y)^3P/(m^2g\mathrm{E})$, which is further expanded as,

$$\mathcal{R} = \mathcal{R}_0 + \sqrt{\mathrm{E}}\mathcal{R}_1 + \mathrm{E}\mathcal{R}_2 + \mathrm{E}^{3/2}\log(32\mathrm{E})\mathcal{R}_{30} + \mathrm{E}^{3/2}\mathcal{R}_{31} + \mathrm{O}(\mathrm{E}^2), \tag{2.32}$$

where $\mathcal{R}_0 = 4\sqrt{2}(c_0-2y)$, $\mathcal{R}_1 = 4\sqrt{2}(c_1+6\sqrt{2}y)$, $\mathcal{R}_2 = 4\sqrt{2}c_2$, $\mathcal{R}_{30} = 4\sqrt{2}c_{30}$ and $\mathcal{R}_{31} = 4\sqrt{2}c_{31}$, where the 32 is retained in the log term in (2.32) for convenience. The boundary conditions are given by,

$$\xi^i(y=0) = 1 \tag{2.33}$$

$$\begin{aligned}\frac{d\xi^i}{dy}\Big(y=0\Big) = (m-1)\sqrt{\mathrm{E}}\Bigg\{ & \frac{\sqrt{2}}{c_0} - \frac{\sqrt{2}c_1\sqrt{\mathrm{E}}}{c_0^2} + \frac{\sqrt{2}\left(c_1^2 - c_0c_2\right)\mathrm{E}}{c_0^3} - \frac{\sqrt{2}\left(c_1^3 - 2c_0c_1c_2 + c_0^2c_{31}\right)\mathrm{E}^{3/2}}{c_0^4} -\\ & \frac{\sqrt{2}c_{30}\mathrm{E}^{3/2}\log(32\mathrm{E})}{c_0^2} + \ldots\Bigg\}\end{aligned} \tag{2.34}$$

$\xi^i(y)$ can thus be expanded as,

$$\begin{aligned}\xi^i(y) = {}& \xi_0^i(y) + \sqrt{\mathrm{E}}\,\xi_1^i(y) + \mathrm{E}\,\xi_2^i(y) + \mathrm{E}^{3/2}\,\xi_3^i(y)\\ & + \mathrm{E}^2\log(32\mathrm{E})\,\xi_{40}^i(y) + \mathrm{E}^2\,\xi_{41}^i(y) + \mathrm{O}(\mathrm{E}^{5/2}) + \mathrm{O}(g\sqrt{\mathrm{E}}),\end{aligned} \tag{2.35}$$

where the leading order radial displacement is now $\mathrm{O}(1)$. Importantly, as already argued in the main text, the RHS in (2.31) is transcendentally small (on account of g), and may therefore be neglected to all algebraic orders considered below. Thus, at $\mathrm{O}(1)$, one obtains,
Finally, at $\mathrm{O}(1)$ we obtain,

$$\frac{d}{dy}\left[\mathcal{R}_0\frac{d\xi_0^i}{dy}\right] = 0, \tag{2.36}$$

with $\xi_0^i(y=0)=1$ and $\dfrac{d\xi_0^i}{dy}(y=0)=0$, which gives

$$\xi_0^i(y)=1. \tag{2.37}$$

At $O(E^{1/2})$ we obtain,

$$\frac{d}{dy}\left[\mathcal{R}_0\frac{d\xi_1^i}{dy}\right]=0, \tag{2.38}$$

with $\xi_1^i(y=0)=0$ and $\dfrac{d\xi_1^i}{dy}(y=0)=\dfrac{\sqrt{2}(m-1)}{c_0}$, which gives,

$$\xi_1^i(y)=-\frac{(m-1)}{\sqrt{2}}\log\left(\frac{c_0-2y}{c_0}\right). \tag{2.39}$$

At $O(E)$ we obtain,

$$\frac{d}{dy}\left[\mathcal{R}_0\frac{d\xi_2^i}{dy}\right]=-\frac{d}{dy}\left[\mathcal{R}_1\frac{d\xi_1^i}{dy}\right], \tag{2.40}$$

with $\xi_2^i=0$ and $\dfrac{d\xi_2^i}{dy}=-\dfrac{\sqrt{2}(m-1)c_1}{c_0^2}$, which gives,

$$\xi_2^i(y)=-3(m-1)\log\left(\frac{c_0-2y}{c_0}\right)-\frac{(m-1)}{2}(\sqrt{2}c_1+6c_0)\left\{\frac{1}{c_0-2y}-\frac{1}{c_0}\right\}. \tag{2.41}$$

At $O(E^{3/2})$ we obtain,

$$\frac{d}{dy}\left[\mathcal{R}_0\frac{d\xi_3^i}{dy}\right]=-\frac{d}{dy}\left[\mathcal{R}_1\frac{d\xi_2^i}{dy}\right]-\frac{d}{dy}\left[\mathcal{R}_2\frac{d\xi_1^i}{dy}\right], \tag{2.42}$$

with $\xi_3^i=0$ and $\dfrac{d\xi_3^i}{dy}=\dfrac{\sqrt{2}(m-1)(c_1-c_0c_2)}{c_0^3}$, which gives,

$$\begin{aligned}\xi_3^i(y)=&-9\sqrt{2}(m-1)\log\left(\frac{c_0-2y}{c_0}\right)-\frac{(m-1)}{\sqrt{2}}(c_2+6\sqrt{2}c_1+36c_0)\left\{\frac{1}{c_0-2y}-\frac{1}{c_0}\right\}\\&+\frac{(m-1)}{2\sqrt{2}}(c_1+3\sqrt{(}2)c_0)^2\left\{\frac{1}{(c_0-2y)^2}-\frac{1}{c_0^2}\right\}.\end{aligned} \tag{2.43}$$

At $O(E^2\log(32E))$ we obtain,

$$\frac{d}{dy}\left[\mathcal{R}_0\frac{d\xi_{40}^i}{dy}\right]=-\frac{d}{dy}\left[\mathcal{R}_{30}\frac{d\xi_1^i}{dy}\right], \tag{2.44}$$

with $\xi_{40}^i=0$ and $\dfrac{d\xi_{40}^i}{dy}=-\dfrac{\sqrt{2}(m-1)c_{30}}{c_0^2}$, which gives,

$$\xi_{40}^i(y)=-\frac{(m-1)}{\sqrt{2}}c_{30}\left\{\frac{1}{c_0-2y}-\frac{1}{c_0}\right\}. \tag{2.45}$$

At $O(E^2)$ we obtain,

$$\frac{d}{dy}\left[\mathcal{R}_0\frac{d\xi_{41}^i}{dy}\right]=-\frac{d}{dy}\left[\mathcal{R}_1\frac{d\xi_3^i}{dy}+\mathcal{R}_2\frac{d\xi_2^i}{dy}+\mathcal{R}_{31}\frac{d\xi_1^i}{dy}\right], \tag{2.46}$$

with $\xi^i_{41}=0$ and $\dfrac{d\xi^i_{41}}{dy}=-\dfrac{\sqrt{2}(m-1)(c_1^3-2c_0c_1c_2+c_0^2c_3)}{c_0^4}$, which gives,

$$\begin{aligned}\xi^i_{41}(y)=&-54(m-1)\log\left(\frac{c_0-2y}{c_0}\right)-\frac{(m-1)}{\sqrt{2}}\{c_3+6\sqrt{2}c_2+54(c_1+3\sqrt{2}c_0)\}\left\{\frac{1}{c_0-2y}-\frac{1}{c_0}\right\}\\&+\frac{(m-1)}{2\sqrt{2}}\{2c_2(c_1+3\sqrt{2}c_0)+9\sqrt{2}(c_1+3\sqrt{(}2)c_0)^2\}\left\{\frac{1}{(c_0-2y)^2}-\frac{1}{c_0^2}\right\}\\&-\frac{(m-1)}{3\sqrt{2}}(c_1+3\sqrt{(}2)c_0)^3\left\{\frac{1}{(c_0-2y)^3}-\frac{1}{c_0^3}\right\}.\end{aligned}\tag{2.47}$$

2.2.4. *Matching*

With the inner and outer boundary layer solutions, and the solution in the outer region, in place, we proceed to derive the necessary constants via matching. To begin with, we expand the far-field solution for small values of $r-1$ by writing it in terms of the outer boundary layer coordinate as $r=1+\sqrt{\mathrm{E}}x$, which leads to the following limiting forms:

$$\mathrm{E}\xi_0^F\sim\sqrt{\mathrm{E}}\frac{\mathcal{B}_0}{2x}\left(1-\frac{\sqrt{\mathrm{E}}x}{2}+O\left(x^2\right)\right),\tag{2.48}$$

$$\begin{aligned}\mathrm{E}^{3/2}\xi_1^F\sim&\,\mathrm{E}\frac{\mathcal{B}_1+4\sqrt{2}\mathcal{B}_0}{2x}\left(1-\frac{\sqrt{\mathrm{E}}x}{2}O\left(x^2\right)\right)+\\&\sqrt{\mathrm{E}}\frac{\sqrt{2}\mathcal{B}_0}{2x^2}\left(1-\sqrt{\mathrm{E}}x+O\left(x^2\right)\right),\end{aligned}\tag{2.49}$$

$$\begin{aligned}\mathrm{E}^2\xi_2^F\sim&\,\mathrm{E}^{3/2}\frac{\mathcal{B}_2+4\sqrt{2}\mathcal{B}_1+32\mathcal{B}_0}{2x}\left(1-\frac{\sqrt{\mathrm{E}}x}{2}+O\left(x^2\right)\right)+\\&\mathrm{E}\frac{2\sqrt{2}\mathcal{B}_1+20\mathcal{B}_0}{4x^2}\left(1-\sqrt{\mathrm{E}}x+O\left(x^2\right)\right)+\\&\sqrt{\mathrm{E}}\frac{4\mathcal{B}_0}{3x^3}\left(1-\sqrt{\mathrm{E}}\frac{3x}{2}+O\left(x^2\right)\right)+\\&8\mathcal{B}_0\mathrm{E}^2\left(\log\sqrt{\mathrm{E}}+\log 2x+\log\left(1+\sqrt{\mathrm{E}}\frac{x}{2}\right)-2\log\left(1+\sqrt{\mathrm{E}}x\right)\right).\end{aligned}\tag{2.50}$$

Next, the outer boundary layer solution needs to be expanded both for large and small x. The large and small x limiting forms are needed for matching with the limiting forms of the outer region and inner boundary layer, respectively. For $x\gg 1$ we obtain the following limiting forms,

$$\xi_0^o\sim\mathcal{G}_{20}+\mathcal{G}_{10}\left(\frac{-2\sqrt{2}}{x}+O\left(\frac{1}{x^2}\right)\right),\tag{2.51}$$

$$\xi_1^o\sim\mathcal{G}_{21}+\mathcal{G}_{11}\left(\frac{-2\sqrt{2}}{x}+O\left(\frac{1}{x^2}\right)\right),\tag{2.52}$$

$$\xi_2^o \sim \mathcal{G}_{22} + 2\mathcal{G}_{10} + \mathcal{G}_{12}\left(\frac{-2\sqrt{2}}{x} + O\left(\frac{1}{x^2}\right)\right) - \mathcal{G}_{10}\frac{x}{\sqrt{2}} - \mathcal{G}_{10}\left(\frac{16\sqrt{2}}{x} + O\left(\frac{1}{x^2}\right)\right), \tag{2.53}$$

$$\xi_3^o \sim \left(-2\sqrt{2}\mathcal{G}_{13} - 12\mathcal{G}_{12} - 16\sqrt{2}\mathcal{G}_{11} + 64\mathcal{G}_{10}\right)\frac{1}{x} + \left(\mathcal{G}_{23} + 2\mathcal{G}_{11} - 10\sqrt{2}\mathcal{G}_{10}\right) + \left(-3\mathcal{G}_{10} - \mathcal{G}_{11}\frac{1}{\sqrt{2}} + 4\mathcal{G}_{10}\right)x - 32\sqrt{2}\mathcal{G}_{10}\log x + O\left(\frac{1}{x^2}\right). \tag{2.54}$$

In the limit $g \ll x \ll 1$, one needs to account for the multi-valuedness of the logarithm in the $\log(x - 2\sqrt{2})$ term (see (2.22)). Here, $x = 2\sqrt{2}$ denotes the singularity of the forward travelling shear wave in the limit of neutral stability. For x crossing $2\sqrt{2}$ along the real axis, there is an ambiguity in the sign of the phase jump associated with the logarithm, an aspect familiar from inviscid hydrodynamic stability (Drazin & Reid 1981). The resolution lies in recognizing that the singularity associated with the unstable mode must lie in the complex plane, so that $x = 2\sqrt{2} - i\epsilon$ ($\epsilon > 0$), even if the displacement from the real axis (ϵ) is transcendentally small. This resolves the sign of the phase jump; the logarithmic term is now $\log(x - 2\sqrt{2} + i\epsilon)$, which leads to a phase jump of $i\pi$ in the limit $x \ll 1$. With this in place, one obtains the following small-x forms for the outer boundary layer solutions:

$$\xi_0^o \sim \mathcal{G}_{10}\left(\log 2\sqrt{2} - \log x + i\pi\right), \tag{2.55}$$

$$\xi_1^o \sim \mathcal{G}_{21} + \mathcal{G}_{11}\left(\log 2\sqrt{2} - \log x + i\pi\right), \tag{2.56}$$

$$\xi_2^o \sim \mathcal{G}_{22} + 10\mathcal{G}_{10} + \mathcal{G}_{12}\left(\log 2\sqrt{2} - \log x + i\pi\right), \tag{2.57}$$

$$\xi_{31}^o \sim \tilde{\mathcal{G}}_{23} + \tilde{\mathcal{G}}_{13}\left(\log 2\sqrt{2} - \log x + i\pi\right), \tag{2.58}$$

$$\xi_3^o \sim \mathcal{G}_{23} - 26\sqrt{2}\mathcal{G}_{10} + 10\mathcal{G}_{11} + \left(\mathcal{G}_{13} + 3\sqrt{2}\mathcal{G}_{12}\right)\left(\log 2\sqrt{2} - \log x + i\pi\right) - 32\sqrt{2}\mathcal{G}_{10}\left(\log 2\sqrt{2} + i\pi\right). \tag{2.59}$$

Finally, the inner boundary layer solution is expanded for large values of y and towards this end, is written in terms of the outer boundary layer coordinate, $y = x/g$ with $x \sim$ O(1) and $g \ll 1$. The multi-valuedness of the logarithmic is again accounted for by noting that the backward travelling shear-wave must lie at $y = c_0/2 - i\epsilon'$ ($\epsilon' > 0$), which leads to a logarithmic term of the form $\log(c_0 - 2y - 2i\epsilon')$ in (2.39) for instance. This in turn leads to a phase jump of $-i\pi$ across $y = c_0/2$. The large-y forms of the inner boundary layer solutions are given by:

$$\xi_0^i \sim 1, \tag{2.60}$$

$$\xi_1^i \sim -\frac{m-1}{\sqrt{2}}\left(\log x + \log\left(\frac{2}{c_0}\right) - \log g - i\pi\right), \tag{2.61}$$

$$\xi_2^i \sim -3\,(m-1)\left(\log x + \log\left(\frac{2}{c_0}\right) - \log g - i\pi\right) + \frac{m-1}{\sqrt{2}}\left(\sqrt{2}\frac{c_1}{c_0} + 6\right), \quad (2.62)$$

$$\xi_3^i \sim -9\sqrt{2}\,(m-1)\left(\log x + \log\left(\frac{2}{c_0}\right) - \log g - i\pi\right) + \frac{m-1}{\sqrt{2}}\left(\frac{c_2}{c_0} + 6\sqrt{2}\frac{c_1}{c_0} + 36\right) - \frac{m-1}{2\sqrt{2}}\left(\frac{c_1}{c_0} + 3\sqrt{2}\right)^2, \quad (2.63)$$

$$\xi_{40}^i \sim \frac{m-1}{\sqrt{2}}\frac{c_{30}}{c_0}, \quad (2.64)$$

$$\xi_{41}^i(y) \sim -54(m-1)\left(\log x + \log\left(\frac{2}{c_0}\right) - \log g - i\pi\right) + \frac{(m-1)}{\sqrt{2}c_0}\{c_{31} + 6\sqrt{2}c_2 + 54(c_1 + 3\sqrt{2}c_0)\} - \frac{(m-1)}{2\sqrt{2}c_0^2}\{2c_2(c_1 + 3\sqrt{2}c_0) + 9\sqrt{2}(c_1 + 3\sqrt{(}2)c_0)^2\} - \frac{(m-1)}{3\sqrt{2}c_0^3}(c_1 + 3\sqrt{(}2)c_0)^3. \quad (2.65)$$

Having determined the appropriate limiting forms, we proceed to match the appropriate terms. In matching (2.60-2.65) to (2.55-2.59), an inconsistency appears in that the only term at O(1) is that from the inner boundary layer (ξ_0^i in (2.60)), and there are no terms for this to match on to, in the outer boundary layer solutions. The resolution involves recognizing that one of the terms at $\mathrm{O}(\sqrt{\mathrm{E}})$, the one proportional to $\log g$ in (2.61), jumps order to cancel the aforementioned O(1) contribution. This implies,

$$g = e^{-\frac{1}{(m-1)}\sqrt{\frac{2}{\mathrm{E}}}}, \quad (2.66)$$

and confirms the transcendental smallness of g anticipated earlier. Owing to this transcendental smallness, the $\log g$ term contributes at an algebraic order lower than the nominal one at which it appears. Next, at $\mathrm{O}(\sqrt{\mathrm{E}})$, we first match the $\log x$ terms in the inner and outer boundary layer solutions ((2.61) and (2.55), respectively), to determine the unknown constant ($\mathcal{G}_{10}$) in the outer boundary layer solution as,

$$\mathcal{G}_{10} = \frac{m-1}{\sqrt{2}}. \quad (2.67)$$

The constant terms in the outer boundary layer (2.51) and the outer region (2.48) solutions are matched to determine the unknown constant ($\mathcal{G}_{20}$) in the outer boundary layer solution as,

$$\mathcal{G}_{20} = 0. \quad (2.68)$$

Then we match the constant term in the inner boundary layer (2.61) and the outer boundary layer solutions (2.55), to determine the leading order term in the eigenvalue expansion (c_0) as,

$$c_0 = 4\sqrt{2}e^{\frac{6}{m-1}}. \quad (2.69)$$

Finally, matching the coefficient of the $\frac{1}{x}$ term in the outer boundary layer (2.51) and the outer region (2.48) solutions is used to determine the unknown constant ($\mathcal{B}_0$) in the outer region solution as,

$$\mathcal{B}_0 = -4(m-1). \quad (2.70)$$

This completes the matching at $\mathrm{O}(\sqrt{\mathrm{E}})$. For all higher orders, the matching thus proceeds in the same sequence as above. For instance, at O(E), matching the $\log x$ term from the

inner (2.62) and outer boundary layer solution (2.56) leads to,

$$\mathcal{G}_{11} = 3(m-1). \tag{2.71}$$

Next, matching the constant terms in the outer boundary layer (2.52) and the outer region (2.49) solutions gives,

$$\mathcal{G}_{21} = (m-1). \tag{2.72}$$

Matching the constant term in the inner boundary layer (2.62) and the outer boundary layer solutions (2.56) gives,

$$c_1 = -16e^{\frac{6}{m-1}}. \tag{2.73}$$

Finally, matching the $\frac{1}{x}$ term in the outer boundary layer (2.52) and the outer region (2.49) solutions gives,

$$\mathcal{B}_1 = 0. \tag{2.74}$$

In a similar manner, one determines all unknown constants involved. The results are summarized below:

$$\begin{aligned}
&g = e^{-\frac{1}{(m-1)}\sqrt{\frac{2}{\mathrm{E}}}},\\
&c_0 = 4\sqrt{2}e^{\frac{6}{m-1}},\ c_1 = -16e^{\frac{6}{m-1}},\ c_2 = 8\sqrt{2}e^{\frac{6}{m-1}},\ c_3 = \left(-656\log(2) - 192 - 256i\pi\right)e^{\frac{6}{m-1}}\\
&\mathcal{G}_{20} = 0,\ \mathcal{G}_{10} = \frac{m-1}{\sqrt{2}},\ \mathcal{G}_{21} = (m-1),\ \mathcal{G}_{11} = 3(m-1),\\
&\mathcal{G}_{22} = \frac{3\sqrt{2}(m-1)}{2},\ \mathcal{G}_{12} = 9\sqrt{2}(m-1),\\
&\mathcal{G}_{23} = \frac{81(m-1)}{3} - 34\log(2)(m-1),\ \mathcal{G}_{13} = 0,\\
&\mathcal{B}_0 = -4(m-1),\ \mathcal{B}_1 = 0,\ \mathcal{B}_2 = 0.
\end{aligned} \tag{2.75}$$

As a result, one has the following asymptotic expression for the eigenvalue,

$$\frac{\omega}{m} \sim 1 - \sqrt{\mathrm{E}}\left[\sqrt{8} + e^{-\frac{1}{m-1}\left(\sqrt{\frac{2}{\mathrm{E}}}-6\right)}\left\{2\sqrt{8} - 16\sqrt{\mathrm{E}} + 4\sqrt{8}\mathrm{E} - 128\mathrm{E}^{3/2}\log(32\mathrm{E}) - 64(3+4i\pi)\mathrm{E}^{3/2}\right\}\right], \tag{2.76}$$

which is the same as the expression as that obtained by direct expansion of the exact solution, for small E, in (2.11).

3. Details of the matched asymptotic analysis for the inertio-elastic instability

Here we give the details for the matched asymptotic analysis for the instability that is described in section 3.2 of the main text, and governed by the full equation (3.2) in the main text.

3.1. *Outer region-* $r - 1 \sim O(1)$

To begin with, we study the solution in the region where $r - 1 \sim \mathrm{O}(1)$. One obtains the following equations at successive orders whose solutions are written alongside. At O(E),

$$\frac{d}{dr}\left[r^3 S_0 \frac{d\xi_0^F}{dr}\right] - S_0\xi_0^F r(m^2-1) = 0, \tag{3.1}$$

with $\xi_0^F \to 0$ for $r \to \infty$, which gives $\xi_0^F(r) = \dfrac{\mathcal{B}_0}{r^{m-1}(r^2-1)}$. Similarly, at $\mathrm{O(E^{3/2})}$,

$$\frac{d}{dr}\left[r^3 S_0 \frac{d\xi_1^F}{dr}\right] - S_0 \xi_1^F r(m^2-1) = -\frac{d}{dr}\left[r^3 S_1 \frac{d\xi_0^F}{dr}\right] + S_1 \xi_0^F r(m^2-1), \tag{3.2}$$

with $\xi_1^F \to 0$ for $r \to \infty$, which gives $\xi_1^F(r) = \dfrac{2\sqrt{2}\mathcal{B}_0}{r^{m-1}(r^2-1)^2} + \dfrac{\mathcal{B}_1}{r^{m-1}(r^2-1)}$.

The $\mathcal{B}_i$'s in the above expressions are integration constants which will be determined from matching considerations (see section 3.4). Using the expressions for ξ_0^F and ξ_1^F above, the solution in the outer region, to $\mathrm{O(E^{3/2})}$, may be written as:

$$\xi^F(r) = \mathrm{E}\frac{\mathcal{B}_0}{r^{m-1}(r^2-1)} + \mathrm{E}^{3/2}\left\{\frac{2\sqrt{2}\mathcal{B}_0}{r^{m-1}(r^2-1)^2} + \frac{\mathcal{B}_1}{r^{m-1}(r^2-1)}\right\} + \mathrm{O(E^2)}. \tag{3.3}$$

In the outer region solution (ξ^F), there are no signatures of the travelling shear-wave singularities. Note that we do not consider the $\mathrm{O(E^2)}$ and higher order contributions to ξ^F since they are not required to determine the growth rate at leading order, an insight that is obtained from the solution of the LHS problem.

3.2. *Outer boundary layer* - $r - 1 \sim O(\sqrt{E})$

We now consider the outer boundary layer using the boundary layer coordinate $x = (r-1)/\sqrt{\mathrm{E}}$. One obtains the following equations at successive orders whose solutions are written alongside.
At $\mathrm{O(E^{1/2})}$ we obtain,

$$\frac{d}{dx}\left[\mathcal{Q}_0 \frac{d\xi_0^o}{dx}\right] = 0 \tag{3.4}$$

$$\Rightarrow\ \xi_0^o(x) = \mathcal{G}_{10} + \mathcal{G}_{11}\log\left(\frac{x-2\sqrt{2}}{x}\right). \tag{3.5}$$

In $\xi_0^o(x)$ above, and in the solutions at higher orders below, the forward and backward travelling wave singularities correspond to $x = 2\sqrt{2}$ and $x = 0$, respectively; the latter location is the edge of the core, since transcendentally small terms are now neglected.
At O(E) we obtain,

$$\frac{d}{dx}\left[\mathcal{Q}_0 \frac{d\xi_1^o}{dx}\right] = -\frac{d}{dx}\left[\mathcal{Q}_1 \frac{d\xi_0^o}{dx}\right], \tag{3.6}$$

$$\Rightarrow\ \xi_1^o(x) = \mathcal{G}_{21} + \mathcal{G}_{11}\log\left(\frac{x-2\sqrt{2}}{x}\right). \tag{3.7}$$

Note that ξ_1^o is again the homogeneous solution since $\mathcal{Q}_1$ has the same x-dependence as $\mathcal{Q}_0$. At $\mathrm{O(E^{3/2})}$ we obtain,

$$\frac{d}{dx}\left[\mathcal{Q}_0 \frac{d\xi_2^o}{dx}\right] = -\frac{d}{dx}\left[\mathcal{Q}_1 \frac{d\xi_1^o}{dx}\right] - \frac{d}{dx}\left[\mathcal{Q}_2 \frac{d\xi_0^o}{dx}\right] + (m^2-1)\mathcal{Q}_0\xi_0^o, \tag{3.8}$$

$$\Rightarrow\ \xi_2^o(x) = \mathcal{G}_{22} + \mathcal{G}_{12}\log\left(\frac{x-2\sqrt{2}}{x}\right) - \frac{\mathcal{G}_{10}}{\sqrt{2}}\left(\frac{32}{x-2\sqrt{2}} + x - 2\sqrt{2}\right) - \mathcal{G}_{10}(m^2-1)\int \frac{x^2-3\sqrt{2}x}{3(x-2\sqrt{2})}\log(x)\,dx$$
$$+ \mathcal{G}_{10}(m^2-1)\int\left(\frac{x^2-3\sqrt{2}x}{3(x-2\sqrt{2})} + \frac{8\sqrt{2}}{3x(x-2\sqrt{2})}\right)\log\left(x-2\sqrt{2}\right)dx$$
$$- \mathcal{G}_{10}(m^2-1)\left(\frac{\sqrt{2}x}{3} - \frac{4}{3}\log\left(\frac{x-2\sqrt{2}}{x}\right)\right). \tag{3.9}$$

At O(E^2) we obtain,

$$\frac{d}{dx}\left[\mathcal{Q}_0\frac{d\xi_3^o}{dx}\right] = -\frac{d}{dx}\left[\mathcal{Q}_1\frac{d\xi_2^o}{dx}\right] - \frac{d}{dx}\left[\mathcal{Q}_2\frac{d\xi_1^o}{dx}\right] - \frac{d}{dx}\left[\mathcal{Q}_3\frac{d\xi_0^o}{dx}\right] + (m^2-1)\mathcal{Q}_1\xi_0^o - 2x(m^2-1)\mathcal{Q}_0\xi_0^o + (m^2-1)\mathcal{Q}_0\xi_1^o, \tag{3.10}$$

$$\Rightarrow\ \xi_3^o(x) = \mathcal{G}_{23} + \mathcal{G}_{13}\log\left(\frac{x-2\sqrt{2}}{x}\right)$$
$$+ 3\sqrt{2}\mathcal{G}_{12}\log\left(\frac{x-2\sqrt{2}}{x}\right) - 3\mathcal{G}_{10}\left(x + \frac{32}{x-2\sqrt{2}}\right) - \frac{\mathcal{G}_{11}}{\sqrt{2}}\left(\frac{32}{x-2\sqrt{2}} + x - 2\sqrt{2}\right)$$
$$+ \frac{\mathcal{G}_{10}}{\sqrt{2}}\left(\frac{(x-2\sqrt{2})^2}{2} + 6\sqrt{2}\left(x-2\sqrt{2}\right) - 64\log\left(x-2\sqrt{2}\right) + \frac{160\sqrt{2}}{x-2\sqrt{2}}\right)$$
$$- (\mathcal{G}_{11}-3\mathcal{G}_{10})(m^2-1)\int\frac{x^2-3\sqrt{2}x}{3(x-2\sqrt{2})}\log(x)\,dx$$
$$+ (\mathcal{G}_{11}-3\mathcal{G}_{10})(m^2-1)\int\left(\frac{x^2-3\sqrt{2}x}{3(x-2\sqrt{2})} + \frac{8\sqrt{2}}{3x(x-2\sqrt{2})}\right)\log\left(x-2\sqrt{2}\right)dx$$
$$- (\mathcal{G}_{11}-3\mathcal{G}_{10})(m^2-1)\left(\frac{\sqrt{2}x}{3} - \frac{4}{3}\log\left(\frac{x-2\sqrt{2}}{x}\right)\right)$$
$$+ \frac{1}{3}(m^2-1)\mathcal{G}_{21}\left(\frac{x^2}{2} - \sqrt{2}x - 4\log\left(x-2\sqrt{2}\right)\right)$$
$$+ \frac{\sqrt{2}}{3}(m^2-1)\mathcal{G}_{10}\left(\frac{x^2}{2} + \sqrt{2}x - 4\log\left(x-2\sqrt{2}\right)\right)$$
$$+ \mathcal{G}_{10}(m^2-1)\int\frac{3x^3-8\sqrt{2}x^2}{6(x-2\sqrt{2})}\log(x)\,dx$$
$$- \mathcal{G}_{10}(m^2-1)\int\left(\frac{3x^3-8\sqrt{2}x^2}{6(x-2\sqrt{2})} + \frac{32}{3x(x-2\sqrt{2})}\right)\log\left(x-2\sqrt{2}\right)dx. \tag{3.11}$$

3.3. *Inner boundary layer - $r-1 \sim O(g\sqrt{E})$*

Finally, we introduce an inner boundary layer in an exponentially small neighborhood of the core, corresponding to O(1) values of the boundary layer coordinate $y = (r-1)/g\sqrt{\mathrm{E}}$ with $g, \mathrm{E} \ll 1$. We have the following equations (and boundary conditions) and solutions at successive orders.

At O(1) we obtain,

$$\frac{d}{dy}\left[\mathcal{R}_0\frac{d\xi_0^i}{dy}\right] = 0, \tag{3.12}$$

with $\xi_0^i(y=0)=1$ and $\dfrac{d\xi_0^i}{dy}(y=0)=0$, which gives

$$\xi_0^i(y)=1. \tag{3.13}$$

At $\mathrm{O}(\mathrm{E}^{1/2})$ we obtain,

$$\frac{d}{dy}\left[\mathcal{R}_0\frac{d\xi_1^i}{dy}\right]=0, \tag{3.14}$$

with $\xi_1^i(y=0)=0$ and $\dfrac{d\xi_1^i}{dy}(y=0)=\dfrac{\sqrt{2}(m-1)}{c_0}$, which gives,

$$\xi_1^i(y)=-\frac{(m-1)}{\sqrt{2}}\log\left(\frac{c_0-2y}{c_0}\right). \tag{3.15}$$

From the expression for $\xi_1^i(y)$ and the solutions at higher orders below, we see that the singularity associated with the backward travelling shear-wave is now resolved, and corresponds to $y=c_0/2$ ($x=gc_0/2$), where c_0 still needs to be determined.
At $\mathrm{O}(\mathrm{E})$ we obtain,

$$\frac{d}{dy}\left[\mathcal{R}_0\frac{d\xi_2^i}{dy}\right]=-\frac{d}{dy}\left[\mathcal{R}_1\frac{d\xi_1^i}{dy}\right], \tag{3.16}$$

with $\xi_2^i=0$ and $\dfrac{d\xi_2^i}{dy}=-\dfrac{\sqrt{2}(m-1)c_1}{c_0^2}$, which gives,

$$\xi_2^i(y)=-3(m-1)\log\left(\frac{c_0-2y}{c_0}\right)-\frac{(m-1)}{2}(\sqrt{2}c_1+6c_0)\left\{\frac{1}{c_0-2y}-\frac{1}{c_0}\right\}. \tag{3.17}$$

3.4. *Matching*

With the inner, outer boundary layer and far-field solutions in place, we proceed to derive the necessary constants via matching appropriate limiting forms of the solutions to each other. First, we expand the outer region solutions for small values of $r-1$, writing it in terms of the outer boundary layer coordinate, $x=(r-1)/\sqrt{\mathrm{E}}$,

$$\mathrm{E}\xi_0^F\sim\sqrt{\mathrm{E}}\frac{\mathcal{B}_0}{2x}\left(1-\frac{\sqrt{\mathrm{E}}x}{2}(2m-1)+O\left(x^2\right)\right), \tag{3.18}$$

$$\mathrm{E}^{3/2}\xi_1^F\sim\mathrm{E}\frac{\mathcal{B}_1}{2x}\left(1-\frac{\sqrt{\mathrm{E}}x}{2}(2m-1)O\left(x^2\right)\right)+\sqrt{\mathrm{E}}\frac{\sqrt{2}\mathcal{B}_0}{2x^2}\left(1-m\sqrt{\mathrm{E}}x+O\left(x^2\right)\right). \tag{3.19}$$

Next, the outer boundary layer solution is expanded both for large and small x for matching with the far-field and inner boundary layer, respectively. For $x\gg 1$,

$$\xi_0^o\sim\mathcal{G}_{20}+\mathcal{G}_{10}\left(\frac{-2\sqrt{2}}{x}+O\left(\frac{1}{x^2}\right)\right), \tag{3.20}$$

$$\xi_1^o\sim\mathcal{G}_{21}+\mathcal{G}_{11}\left(\frac{-2\sqrt{2}}{x}+O\left(\frac{1}{x^2}\right)\right), \tag{3.21}$$

and

$$\xi_2^o \sim \mathcal{G}_{22} + 2\mathcal{G}_{10} + \mathcal{G}_{12}\left(\frac{-2\sqrt{2}}{x} + O\left(\frac{1}{x^2}\right)\right) - \mathcal{G}_{10}\frac{x}{\sqrt{2}}$$
$$-\mathcal{G}_{10}\left(\frac{16\sqrt{2}}{x} + O\left(\frac{1}{x^2}\right)\right) + \mathcal{G}_{10}(m^2-1)\left(\frac{-\sqrt{2}x}{3} + \frac{8\sqrt{2}}{3x}\right)$$
$$+\frac{4}{3}\mathcal{G}_{10}(m^2-1)\left(1 + \mathcal{Z}_1 + \mathcal{Z}_2 + \log(2\sqrt{2})(\log(2\sqrt{2}) - \log(i\gamma))\right), \quad (3.22)$$

where $\mathcal{Z}_1$ and $\mathcal{Z}_2$ are real constants defined by the integrals,

$$\mathcal{Z}_1 = \int_{2\sqrt{2}}^{\infty} \frac{\log(x-2\sqrt{2}) - \log(x)}{x} dx, \quad (3.23)$$

$$\mathcal{Z}_2 = \int_{2\sqrt{2}}^{\infty} \frac{2\sqrt{2}\log x - 2\sqrt{2}\log 2\sqrt{2}}{x(x-2\sqrt{2})} dx. \quad (3.24)$$

The integrals in the exact expression, (3.9), for ξ_2^o appear to have a singularity when taking the limit $x \gg 1$. To resolve this, we again recognize that the travelling wave singularity must be displaced into the complex plane for an unstable mode and the constant γ indicates this small but finite displacement. Note that the last term in (3.22) when combined with the constant $\mathcal{G}_{22}$ (the first term), shows that ξ_2^o is independent of the arbitrary constant γ, which is only used as an intermediate step.

For $gc_0 \ll x \ll 1$,

$$\xi_0^o \sim \mathcal{G}_{10}\left(\log 2\sqrt{2} - \log x + \phi\right), \quad (3.25)$$

$$\xi_1^o \sim \mathcal{G}_{21} + \mathcal{G}_{11}\left(\log 2\sqrt{2} - \log x + \phi\right), \quad (3.26)$$

$$\xi_2^o \sim \mathcal{G}_{22} + 10\mathcal{G}_{10} + \mathcal{G}_{12}\left(\log 2\sqrt{2} - \log x + \phi\right)$$
$$-\frac{4}{3}\mathcal{G}_{10}(m^2-1)\left(\log 2\sqrt{2} - \log x + \phi\right)$$
$$+\mathcal{G}_{10}(m^2-1)\left(\frac{2}{3} + \frac{4}{3}(\mathcal{Z}_3 - \mathcal{Z}_4) - \frac{4}{3}\log(x)(\phi + \log(2\sqrt{2}))\right)$$
$$+\mathcal{G}_{10}(m^2-1)\left(\frac{8}{3}\log 2\sqrt{2}(\Phi_1 + \log 2\sqrt{2}) - \frac{4}{3}\log(2\sqrt{2})\log(i\gamma)\right), \quad (3.27)$$

where $\mathcal{Z}_3$ and $\mathcal{Z}_4$ are real constants defined by the integrals

$$\mathcal{Z}_3 = \int_0^{2\sqrt{2}} \frac{\log(2\sqrt{2}-x) - \log 2\sqrt{2}}{x} dx, \quad (3.28)$$

and

$$\mathcal{Z}_4 = \int_0^{2\sqrt{2}} \frac{\log x - \log 2\sqrt{2}}{x - 2\sqrt{2}} dx. \quad (3.29)$$

The inner boundary layer solution is written in terms of the outer boundary layer coordinate, using $y = x/g$, and then expanded for $g \ll 1$ (corresponding to $y \gg 1$) as,

$$\xi_0^i \sim 1,$$

$$\xi_1^i \sim -\frac{m-1}{\sqrt{2}}\left(\log x + \log\left(\frac{2}{c_0}\right) - \log g + \phi'\right), \tag{3.30}$$

$$\xi_2^i \sim -3\,(m-1)\left(\log x + \log\left(\frac{2}{c_0}\right) - \log g + \phi'\right) + \frac{m-1}{\sqrt{2}}\left(\sqrt{2}\frac{c_1}{c_0} + 6\right). \tag{3.31}$$

At O(1), we note that the only term contributing is from the inner boundary layer. Thus to achieve a consistent balance, a term from the eigenfunction at $\mathrm{O}\left(\sqrt{\mathrm{E}}\right)$ must contribute. This gives,

$$g = e^{-\frac{1}{(m-1)}\sqrt{\frac{2}{\mathrm{E}}}}. \tag{3.32}$$

This implies that the $\log g$ term contributes at a lower order as opposed to the order in which it appears in the inner-boundary layer expansion.

The growth rate only results at $\mathrm{O}(\mathrm{E}^2)$. By looking at the lower order matching results, it is evident that only the functional form of $\log\left(x - 2\sqrt{2}\right)$, and not $\log\left(x - 2\sqrt{2}\right) - \log x$, results in an imaginary part for the eigenvalue. Such a form only occurs at $\mathrm{O}(\mathrm{E}^2)$. This is also evident in the calculation that is carried out for the LHS problem earlier. Thus, one may directly carry out the matching procedure for the imaginary term at $\mathrm{O}(\mathrm{E}^2)$ between the inner and outer boundary layer solutions. The eigenvalue constant, c_3, enters the inner boundary layer solution at $\mathrm{O}(\mathrm{E}^2)$ and writing $c_3 = c_{3r} + ic_{3i}$, gives immediately an expression for the growth rate (c_{3i}):

$$\frac{(m-1)c_{3i}}{\sqrt{2}c_0} = -32\sqrt{2}\pi\mathcal{G}_{10} - \frac{4}{3}(m^2-1)\pi\mathcal{G}_{21} - \frac{8\sqrt{2}}{3}(m^2-1)\pi\mathcal{G}_{10}. \tag{3.33}$$

The RHS of (3.33) results from the limiting form of the outer boundary layer solution at $\mathrm{O}(\mathrm{E}^2)$ (3.11). As noted earlier, only terms of the functional form $\log\left(x - 2\sqrt{2}\right)$ in (3.11) contribute to the imaginary part and hence only these are considered when evaluating the limiting form. The matching procedure is detailed in 2.2.4, and to O(E), yields the following expressions for the various constants:

$$c_0 = 4\sqrt{2}e^{\frac{6}{m-1}},\ c_1 = 16(m-2)e^{\frac{6}{m-1}},$$
$$\mathcal{G}_{20} = 0,\ \mathcal{G}_{10} = \frac{m-1}{\sqrt{2}},\ \mathcal{G}_{21} = (2m-1)(m-1),\ \mathcal{G}_{11} = 3(m-1),$$
$$\mathcal{B}_0 = -4(m-1),\ \mathcal{B}_1 = 4\sqrt{2}(m-1)(m-3).$$

These are sufficient to find the growth rate at $\mathrm{O}(\mathrm{E}^2)$. Recall from section 3.3, that the location of the backward travelling shear-wave is given by $y = c_0/2$ in terms of the inner boundary layer coordinate. Using the expression for c_0, we obtain the radial location of the backward travelling shear wave as $r = 1 + 2\sqrt{2\mathrm{E}}e^{-\frac{1}{(m-1)}\sqrt{\frac{2}{\mathrm{E}}}+\frac{6}{m-1}}$. The shear wave is indeed a transcendentally small distance away from the vortex core, as anticipated by the simplistic approach earlier.

Substituting the above results in the growth rate expression yields,

$$c_{3i} = -4\sqrt{2}\pi e^{\frac{6}{m-1}}\left(32\sqrt{2} + \frac{4}{3}(m^2-1)(2m-1) + \frac{8\sqrt{2}}{3}(m^2-1)\right), \tag{3.34}$$

which corresponds to an unstable mode.

REFERENCES

Balmforth, N.J. 1998 Stability of vorticity defects in viscous shear. *J. Fluid Mech.* **357**, 199–224.

Balmforth, N.J. & Morrison, P.J. 1995a *Singular eigenfunctions for shearing fluids I.*. Institute for Fusion studies, University of Texas, Austin, Report No. 692.

Balmforth, NJ, Morrison, PJ & Thiffeault, J-L 2013 Pattern formation in hamiltonian systems with continuous spectra; a normal-form single-wave model. *arXiv preprint arXiv:1303.0065* .

Balmforth, N.J., Smith, S.G. Llewellyn & Young, W.R. 2001 Disturbing vortices. *J. Fluid Mech.* **426**, 95–133.

Case, K.M. 1960 Stability of inviscid plane couette flow. *Phys. Fluids* **3**, 143.

Drazin, P.G. & Reid, W.H. 1981 *Hydrodynamic stability*. Cambridge University Press.

Gakhov, F.D. 1990 *Boundary value prolems*. Dover.

Graham, M. D. 1998 Effect of axial flow on viscoelastic taylor-couette instability. *J. Fluid Mech.* **360**, 341–374.

Pradeep, D.S. & Hussain, F. 2006 Transient growth of perturbations in a vortex column. *J. Fluid Mech.* **550**, 251.

Reddy, J. Sashi Kiran 2015 *The spectrum of the Elastic Rayleigh Equation.*. Masters thesis, Jawaharlal Nehru Centre for Advanced Scientific Research.

Roy, A. & Subramanian, G. 2014*a* An inviscid modal interpretation of the 'lift-up' effect. *J. Fluid Mech.* **757**, 82–113.

Roy, A. & Subramanian, G. 2014*b* Linearized oscillations of a vortex column: the singular eigenfunctions. *J. Fluid Mech.* **741**, 404–460.

Schecter, D.A., Durbin, D.H.D., Cass, A.C., Dritscoll, C.F., Lansky, I.M. & O'Neil, T.M. 2000 Inviscid damping of asymmetries on a two-dimensional vortex. *Phys. Fluids* **12**, 2397.

Slavyanov, S. Yu. & Lay, W. 2000 *Special functions: a unified theory based on singularities*. Oxford.